Class Notes, 31415 RF-Communication Circuits

Chapter VI

OSCILLATORS

Jens Vidkjær

NB234

Contents

VI Oscillators

Most communication system and measurement equipment include oscillators and they are often key components that directly influence system specifications and tolerances. Therefore, oscillator design objectives commonly encompass one or more of the following question in addition to the basic requirement of producing periodic waveshapes.

- Frequency sensitivity and drift in short and long terms
- Waveshapes and Harmonic distortion
- Noise
- Frequency control and adjustment range

To address the fundamental properties in an instructive manner, we shall start considering some prototype oscillator circuits, where the different aspects of oscillator performance may be separately considered. The prototype oscillators are simple because they include transformer-coupled feed-back paths. In practical circuits transformers are often avoided and the feed-back paths may be more difficult to identify.

It is not possible here to cover more than a few of the oscillator circuits that are in practical use. Below we consider and exemplify one very common family of oscillator circuits in some depth. Other oscillator types may be treated equivalently using the approaches that are demonstrated here, so the reader should be able to conduct investigations of other circuits on his own as necessary.

One topic is given more attention here than in most other introductory texts, namely the mechanisms of amplitude control. This is a topic that must be addressed in every oscillator design, but since it is strongly nonlinear, it is often considered as a problem to be dealt with experimentally. Below, however, we benefit from the presentation of nonlinear amplifiers in the foregoing chapter and include amplitude control in the design examples. Also the more advanced problem of amplitude stability is considered but, due to the lengthy calculations, in an appendix.

VI-1 Oscillator Basics

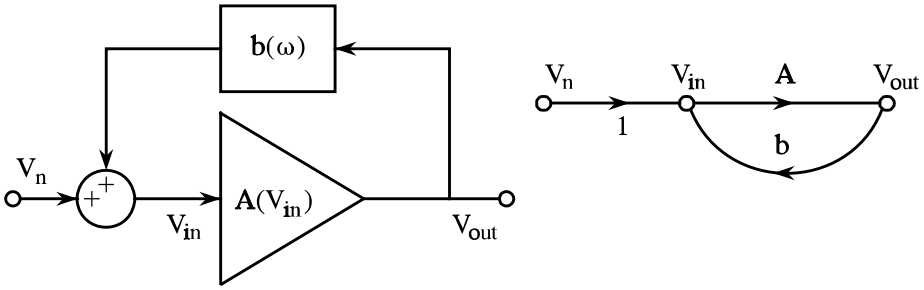

Fig.1 Basic oscillator components and the corresponding signal flow-graph.

Oscillator circuits for sinusoidal oscillations include functions that may be illustrated by the block-diagram of Fig.1. There is a level dependent - i.e. a nonlinear - amplification $A(V_{in})$, which stabilizes the amplitude of oscillation, and a frequency selective positive feedback circuit $b(\omega)$, which determines the frequency of oscillations. Besides the voltage from the feedback loop around the amplifier, an additional input voltage V_n that represents either amplifier noise or a fast decaying signal is inserted. It is required to start oscillations, especially in analytical models or simulations. The voltage transfer function, which is illustrated by the flow-graph, implies

$$\frac{V_{out}}{V_n} = \frac{A}{1 - bA} . \tag{1}$$

Self sustained oscillations are possible at a frequency ω_0 and an amplifier input V_{in0}, where the transfer function above becomes singular. This properties, which implies a loop gain equal to one, is known as Barkhausen's condition,

$$b(\omega_0)\, A(V_{in0}) = 1 . \tag{2}$$

The criterion must be applied in a strictly complex sense so the equation constrains real parts or phasor lengths if, simultaneously, the imaginary parts or the phasor angles are forced to zero. To ensure start of oscillation and subsequently amplitude stabilization, the loop gain must start being greater than one with no amplitude and then decrease monotonously until Barkhausen's criterion is met at the desired amplitude. A characteristic like the one in Fig.2 has this property.

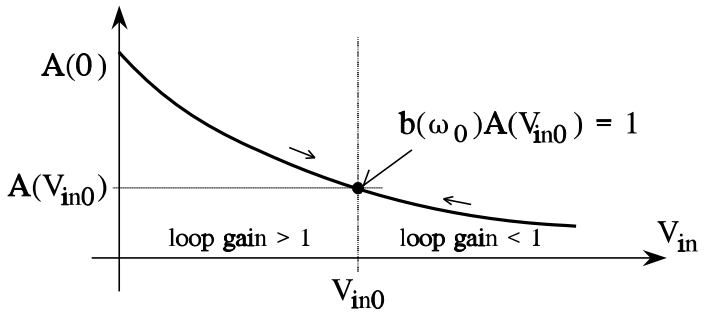

Fig.2 Nonlinear amplifier characteristic for oscillator amplitude stabilization.

Separation into a nonlinear amplifier circuit and a frequency selective feedback network may not be as distinct in practice as suggested by the initial presentation above. Designing oscillators it is important, however, to identify the two functions and assure that they are working properly under influence of each other including the ability to start oscillating at the required frequency. More detailed accounts on such basic questions may be found in ref´s [1],[2].

Prototype Feedback Oscillators

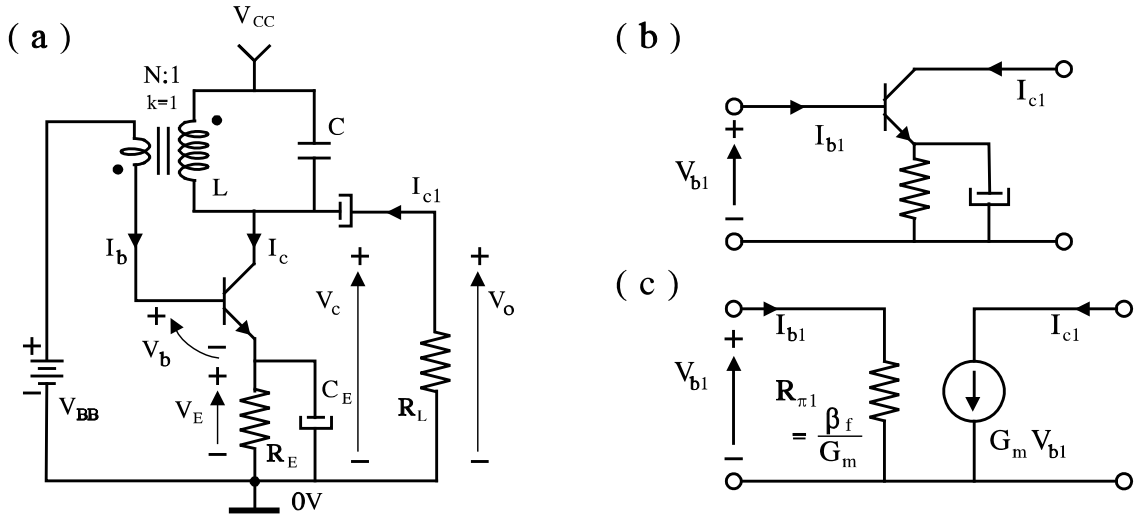

Fig.3 Oscillator circuit with class AB or C amplification (class depends on circuit parameters). The transistor equivalent in (c) assumes no saturation and relates fundamental frequency components.

We shall start our discussion of oscillators by considering simple circuits where the frequency is determined by a parallel resonance circuit, sometimes referred to as the tank-circuit. The tuning inductance is primary winding in a transformer, where feedback is taken from the secondary winding. Candidates for an amplifier are the parallel-tuned large-signal amplifiers with current or resistor biasing or the differential amplifier. They have both decreasing gain with increasing input drive voltage as it was discussed in section 5-3. An oscillator with a single transistor is shown in Fig.3(a), and although a circuit with a separate feed-back winding may be impractical in practice, it is easily understood and it will be a vehicle in the present introductory discussion. Fig.3(c) shows the large signal equivalent circuit for the transistor. Numerical methods were employed in Chap.5 - Eqs.(5-101) through (5-107) -to find the large-signal transconductance G_m, which is a function of the drive level V_{b1}. It was assumed that the transistor operates free of saturation, and that the Q-factor is high enough to ensure a sinusoidal base-emitter voltage around the mean voltage V_{b0},

$$V_b = V_{b0} + V_{b1} \cos \omega_0 t \,. \tag{3}$$

Investigation of Barkhausen's condition in an oscillator circuit may be done as shown by the equivalent circuit in Fig.4, where we - hypothetically - have opened the loop inside the

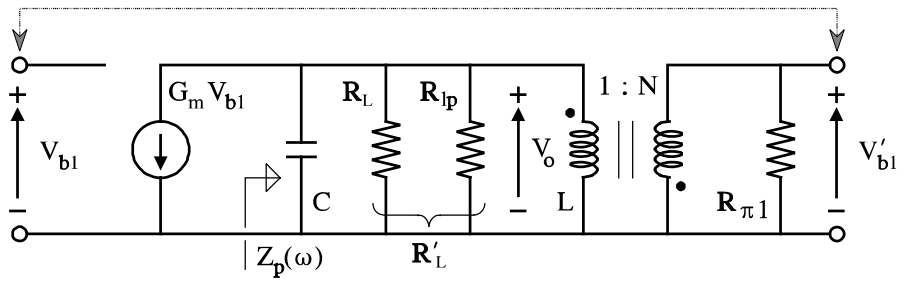

Fig.4 Equivalent circuit for calculating open loop gain. R_{lp} represents possible losses in inductor L. Oscillations are established by connecting the two ports as indicated by the dashed line.

transistor. Connecting input and output ports in this circuit establishes the oscillator with $V_{b1} = V'_{b1}$, a condition that also must apply to the open-loop equivalent circuit, where the condition now reads,

$$V'_{b1} = -G_m(V_{b1})\, Z_p(\omega)\left[-N\right] V_{b1} \ . \tag{4}$$

To get correct sign in the condition, the transformer winding is turned to cancel the sense of G_m in common emitter configuration. The total parallel resistance of Z_p is combined from the external load, R_{LP}, a possible inductor loss, R_{lp}, and the transistor input resistance R_π seen through the transformer, which has winding ratio N. We get

$$R_p = R_L' \left\| \frac{R_\pi}{N^2} \right. , \qquad R_L' = R_L \| R_{lp} \ , \qquad R_{lp} = Q_L\, L\, \omega_0 \ , \tag{5}$$

where Q_L is the Q-factor of the inductor at the resonance frequency ω_0. The impedance of the parallel tuned circuit is expressed

$$Z_p(\omega) = \frac{R_p}{1 + j\, Q_l\, \beta(\omega)} \ , \qquad \textit{where}$$

$$\omega_0 = \frac{1}{\sqrt{L\, C}} \ , \qquad Q_l = R_p\, C\, \omega_0 \ , \qquad \beta(\omega) = \left(\frac{\omega}{\omega_0} - \frac{\omega_0}{\omega} \right). \tag{6}$$

Frequency dependency is here kept in the function $\beta(\omega)$, which was introduced in Chap.II, Eq.II(6). The function, which becomes zero at the resonance frequency, should not be confused with the transistor current gain β_f. The Q-factor Q_l is the loaded Q, which includes all resistances in the resonance circuit. The resonance frequency expression may be considered as the imaginary part of Barkhausen's requirement since at resonance Z_p gets no imaginary part. The condition becomes

$$\frac{V_{b1}'}{V_{b1}} = G_m(V_{b1})\, Z_p(\omega)\, N = 1 \quad \Rightarrow \quad \begin{cases} \textit{imag.condition}: & \omega = \omega_0 = \dfrac{1}{\sqrt{L\,C}}\,, \\ \textit{real condition}: & G_m(V_b)\, R_p\, N = 1\,. \end{cases} \tag{7}$$

Incorporating the relationship between the effective fundamental frequency transconductance and input resistance of the transistor,

$$R_{\pi 1}(V_{b1}) = \frac{\beta_f}{G_m(V_{b1})}\,, \tag{8}$$

we get from the real-part requirement

$$G_m\, R_p\, N = G_m \frac{R_L'\ \beta_f / G_m N^2}{R_L' + \beta_f / G_m N^2}\, N = 1 \quad \Rightarrow \tag{9}$$

$$G_m\, R_L'\, N\,(\,1 - N/\beta_f\,) \approx G_m\, R_L'\, N = 1\,.$$

The last, approximate, expression assumes that the transformer winding ratio over the transistor current gain β_f is small. This will be the common situation with N less than one and current gain significantly greater than one. Observe that the effect of the assumption is to disregard the loading of the resonance circuit by the transistor input resistance.

Had we insisted in a strict identification of the two basic oscillator blocks from Fig.1 in the present circuit, it would be a natural choice to let the center frequency gain represent the level dependent amplifier, and let the feedback through the secondary winding be the frequency selective block, i.e.

$$A(V_{b1}) = -G_m(V_{b1})\, R_p\,, \qquad b(\omega) = \frac{-N}{1 + j Q_l\, \beta(\omega)}\,. \tag{10}$$

We may think in terms of this separation when basic stability and noise properties of oscillators are discussed in subsequent paragraphs.

Instead of employing a limiting amplifier with one transistor in the prototype oscillator, the differential stage could also be used. An example is shown in Figure 5-57.Inserted in (b) is the large signal equivalent circuit of a differential pair from Chap.5, Fig.5-54, now with terminal grounded according to the diagram of the complete oscillator. The total collector current in transistor Q_2 is includes a DC component of approximately half the tail current I_{ET} and the differential current ΔI_c, where, cf. Eqs.(5-140) and (5-141),

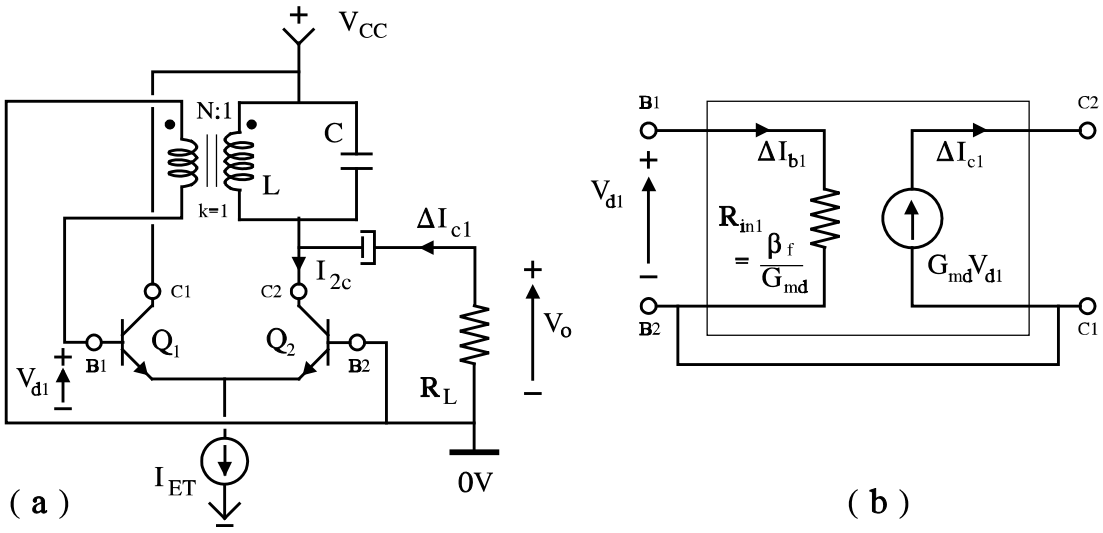

Fig.5 Oscillator circuit with differential amplifier. The equivalent circuit in (b) assumes no saturation and relates fundamental frequency components.

$$I_{2c} \approx \frac{I_{ET}}{2} - \Delta I_c. \tag{11}$$

Compared to the single transistor coupling in Fig.3, the controlled current source has changed direction. This is also the case in the equivalent circuit of Fig.6, which illustrates the loop-gain in Barkhausen's criterion. To compensate the new current source orientation, the sense of the transformer must also be changed in comparison with the single transistor case from Fig.4. Excepts for details in the functions that govern the fundamental frequency transconductances G_m and G_{md} respectively, the equivalent circuits are similar, so with respect to the fulfillment of Barkhausen's criterion we need not consider the differential prototype oscillator separately, but simply use G_{md} in Eq.(9) instead of G_m.

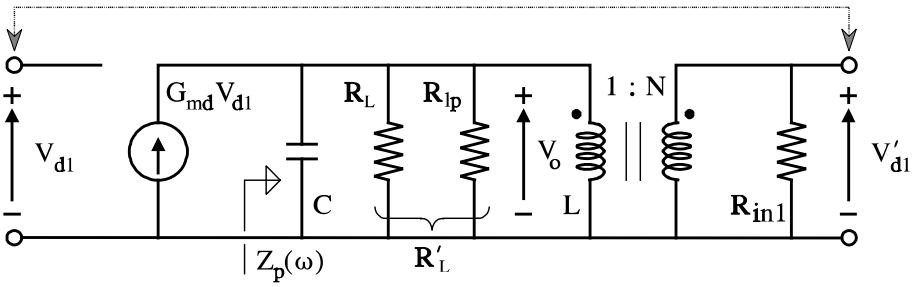

Fig.6 Equivalent circuit for calculating the loop gain in the differential oscillator from Fig.5. R_{lp} represents still possible losses in inductor L.

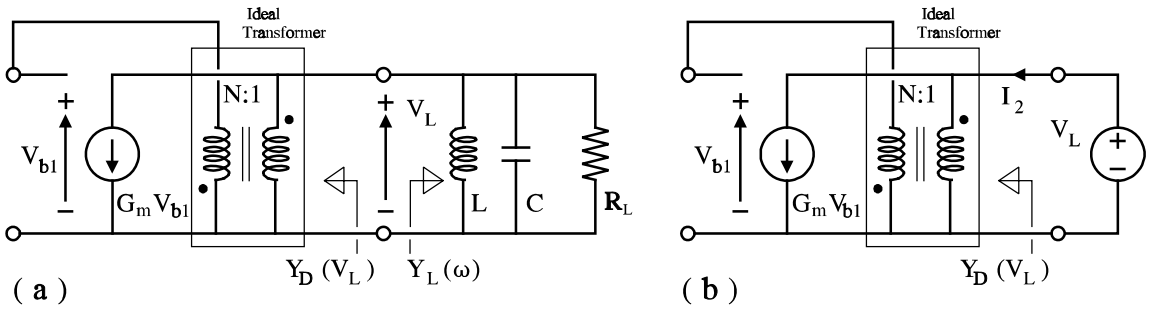

Fig.7 Redrawing of Fig.4 without R_{lp} and $R_{\pi 1}$ (a), illustrating the negative conductance point of view in oscillator design. Negative conductance is found by the setup in (b).

Negative Conductance Criteria

Instead of Barkhausen's criterion, the conditions for oscillation may sometimes be formulated from a negative conductance or negative resistance point of view[1]. In an undamped resonance circuit, oscillation will continue forever at the resonance frequency once they have been started. If power is taken from the circuit by parallel loading through a passive, i.e. positive, conductance, continued oscillation requires continuous supply of power. To maintain the conditions for an undamped resonator, the model of the circuitry that delivers power must contain a conductance in parallel to the load of same size but with negative sign. We may illustrate the method by reformulating the oscillation condition for our prototype oscillator to negative conductance form.

The diagram in Fig.7 holds a simplified version of the oscillator equivalent circuit in Fig.4. Inductor losses and the input resistance of the transistor are disregarded in the new circuit, which is redrawn to emphasis its separation into a passive load, Y_L, paralleled by an active network with device and feed-back components, Y_D. The separating cut is somewhat arbitrary provided that the ohmic parts of the device and the load are at different sides. In Fig.7 we have chosen to let the device admittance be real and frequency independent, a decision that also separates the amplitude control function from the frequency selective network. The parallel admittance of the device may be found as sketched in Fig.7(b), i.e.

$$Y_D = \frac{I_2}{V_L} = G_m(V_{bl})\,\frac{V_{bl}}{V_L}, \qquad V_{bl} = -N\,V_L \qquad \Rightarrow \qquad Y_D = Y_D(V_L) = -N\,G_m\big(N\,V_L\big). \quad (12)$$

It follows from the initial resonance circuit discussion that the admittances - impedances as well - sum to zero at stationary oscillations, i.e.

---

1) Formerly, that sort of considerations were used reversely to avoid oscillations in setting up two-port stability criteria in sec.III-1,p.11.

$$Y_D(V_L) + Y_L(\omega_0) = 0, \qquad where \qquad Y_L(\omega) = \frac{1}{R_L}\left(1 + jQ\,\beta(\omega)\right) \tag{13}$$

Taking real and imaginary parts in the equation above leads to the same requirements as did Barkhausen's criterion in Eq.(7). We get

$$\begin{aligned} &imaginary\ condition: && \frac{Q\beta(\omega)}{R_L} = 0 && \Rightarrow && \omega = \omega_0 = \frac{1}{\sqrt{L\,C}}, \\ &real\ condition: && -N G_m + \frac{1}{R_L} = 0 && \Rightarrow && G_m(V_L)\,R_L\,N = 1. \end{aligned} \tag{14}$$

At microwave frequencies oscillators may be build around diodes that have negative incremental output conductances where the negative conductance approach is appropriate. In most cases there are no advantage of using the method on feedback oscillator couplings, which are our main concern below. Having demonstrated equivalency between the two points of view we shall therefore leave the negative conductance subject. Interested readers may consult refs.[3] or [4] for further discussions and references.

Frequency Stability

Parameter variations due to temperature variations or parameter spreading in production clearly changes the conditions for oscillation. Using logarithmic differentiation, variations of the tuning capacitance or inductance changes the oscillating frequency of the prototype circuit according to

$$\log\omega_0 = \frac{-1}{2}\left[\log C + \log L\right] \qquad \Rightarrow \qquad \frac{\delta\omega_0}{\omega_0} = \frac{-1}{2}\left[\frac{\delta C}{C} + \frac{\delta L}{L}\right]. \tag{15}$$

To keep the oscillating frequency stable under thermal variations we should clearly use tuning elements with small thermal coefficients. Crystals, which are considered in details later, are examples showing extremely small temperature variations. Using conventional components, a simple mean for stabilizing is to chose inductors and capacitors that have relative thermal coefficients of equal size but opposite signs.

The amplifier circuit in the idealization from Fig.1 contributes nothing to the frequency stability of the oscillator. Practical amplifiers, however, include phase-shifts that must be accounted for when Barkhausen´s condition is enforced. Suppose we have an amplifier with a small phase deviation $\Delta\varphi$, i.e.

$$A = \left|A\,(V_{in})\right| e^{-j\Delta\varphi}, \tag{16}$$

If the feedback follows the impedance of a parallel resonance circuit, the frequency of oscillation will differ from the resonance frequency ω_0 to compensate the extra phase

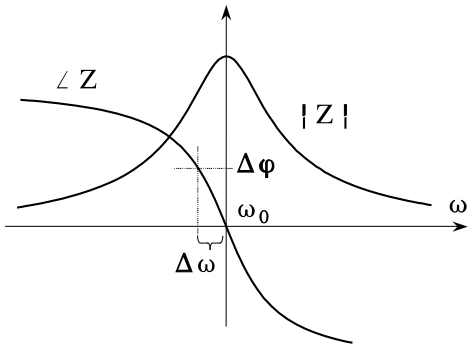

Fig.8 Impedance of a parallel tuned circuit. The steepness of the phase characteristic determines the oscillator frequency sensitivity Δω/Δφ

deviation as indicated by Fig.8. The phase of a parallel tuned circuit is, cf. Eq.(6),

$$\angle b \;=\; \angle Z_p \;=\; -\tan^{-1}\left\{\, Q_l\;\beta(\omega)\,\right\}\,. \tag{17}$$

Thereby, the phase and frequency deviations around resonance become

$$\Delta\angle Z_p \;=\; \left.\frac{d\angle Z_p}{d\omega}\right|_{\omega=\omega_0}\Delta\omega \;=\; -\frac{2\,Q_l}{\omega_0}\;\Delta\omega\;. \tag{18}$$

Barkhausen´s condition requires zero phase-shift around the loop, so to compensate a small amplifier phase-shift, the oscillation frequency must deviate Δω from ω_0, where

$$\Delta\angle Z_p - \Delta\varphi \;=\; 0 \qquad\Rightarrow\qquad \Delta\omega \;=\; -\frac{\omega_0}{2\,Q_l}\;\Delta\varphi\,. \tag{19}$$

This results shows clearly that a high Q-factor in the resonance circuit provides a low influence on the oscillator frequency from the amplifying circuit. The latter may be build from conventional electronic components that are more prone to temperature variations and parameter spreading than the often highly specialized resonator components, which determine frequency and Q. A so-called frequency stability factor S_f are sometimes introduced, where

$$S_F \;\equiv\; \omega_0\left|\frac{d\varphi}{d\omega}\right|_{\omega_0} \;=\; 2\,Q_l\,. \tag{20}$$

In the prototype circuit, the S_f concept is a simple alternative to the Q-factor and seemingly superfluous. There are, however, other oscillator configurations where the association to a Q-factor is not straight-forward. In such cases the frequency stability factor is a meaningful quantity by itself or, alternatively, the derivative of the open-loop gain phase with respect to angular frequency may by used to calculate a Q-factor that indicates frequency stability.

Amplitude Stability

Oscillators with amplitude control of a type that involves the DC bias in the amplifier to adjust gain, may exhibit an amplitude instability problem known as squegging. This is illuminated by Fig.9 that shows simulations on the oscillator circuit in Fig.3, where the DC bias current through the nonlinear driven transistor depends on the signal level. In contrast, the bias current of the differential prototype oscillator from Fig.5 is kept fixed, so this type of problems should not be seen, if the amplifier is well designed. However, this and many other oscillator circuits may still exhibit amplitude instabilities if the amplitude control is not well planned, so transistors are forced into unintentional saturation or secondary breakdown, which may provide unexpected bias variations.

Like many other analog large-signal nonlinear circuit problems, it is difficult to conduct simple analytical investigations of the oscillator amplitude stability and to get results that are suitable in design. Even simple cases become rather lengthy and involved so we refer to Appendix VI-A, which discusses amplitude stability in the single transistor prototype oscillator. In brief, it is demonstrated that to avoid squegging, the time constant in the bias adjustment - in turns the gain regulation - should be of comparable length to the time constant by which oscillation may build up or decay across the resonance circuit, i.e. the logarithmic decrement that was introduced by Eq.II(30) in section II-1.

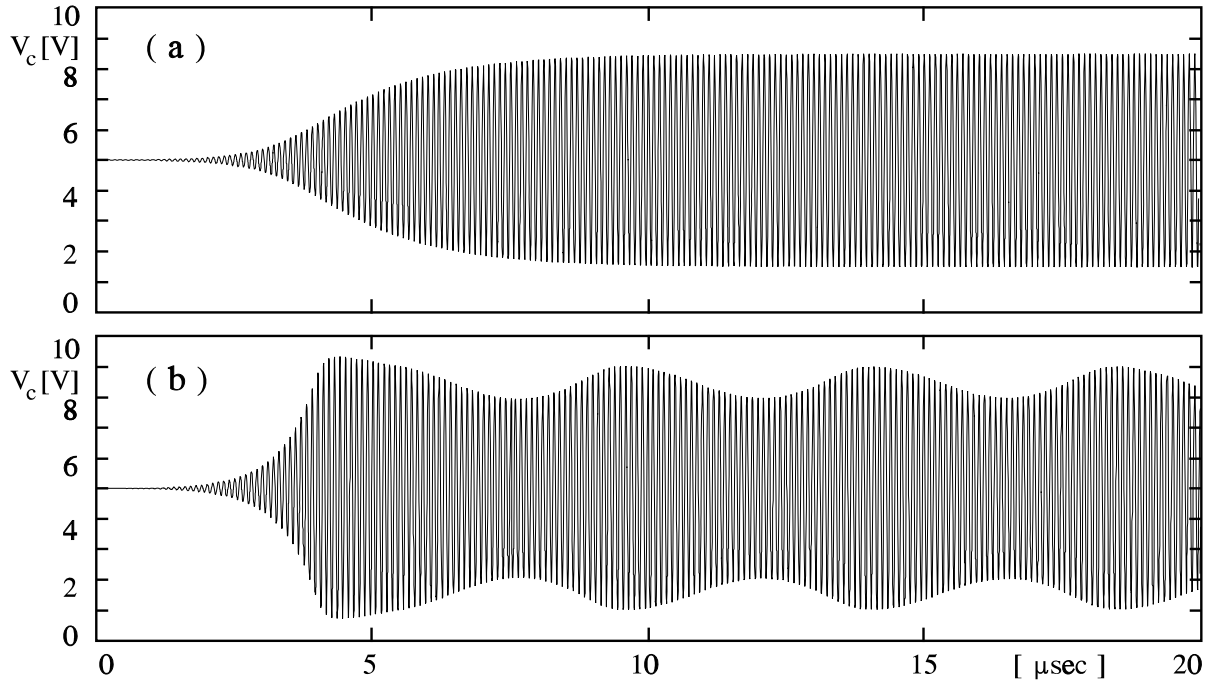

Fig.9 Prototype oscillator outputs, (a) stable amplitude, τ_E/τ_Q=1, and (b) instability for τ_E/τ_Q=4.5 (details in Appendix VI-A).

Oscillator Noise

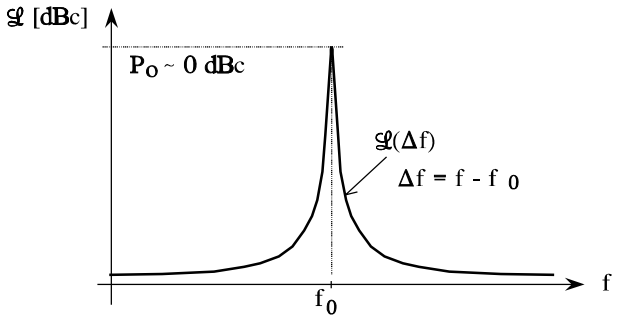

Fig.10 Spectrum analyzer output from an oscillator. $\mathcal{L}(\Delta f)$ is called the single sideband noise function. The widening of the spectrum around the center frequency is caused by noise.

Noise in oscillators manifests itself by an output spectrum that is not just a single line but gives spectrum that widens apart from the center frequency as sketched in Fig.10. We shall consider a simplified, partly empirical oscillator noise model, the so-called Leeson model [5], in this section. The model explains major noise properties and parameter dependencies in experimental observations. The prototype oscillators from above are used to make the simplified model plausible, but due to the nonlinear amplifier operation in an oscillator, the detailed theoretical treatment of oscillator noise is complex and far beyond our scope. To go further, the interested reader should consult ref´s [6] or [7],sec.10.4.

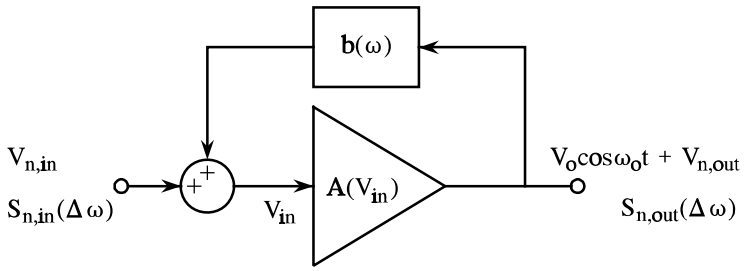

Fig.11 Oscillator block-scheme for noise description.

The oscillator noise model is obtained in two steps. It is assumed that the noise can be ascribed to the amplifier and represented by an equivalent input noise. First the relationship between input and output noise spectra are calculated. Second, the nature and shape of the actual noise source spectra are incorporated.

Fig.11 repeats out initial block scheme representation of an oscillator. Applied to the prototype oscillator, the subdivision from Eq.(10) implies that the frequency selective feedback network holds lossless components L and C only. All noise sources are represented by the input noise voltage $V_{n,in}$. When the oscillator is running, the output contains both the desired constant amplitude sinusoidal voltage $V_o\cos\omega_0 t$ and noise components $V_{n,out}$, which

originates from $V_{n,in}$. We suppose initially that all noise voltages are so small that they have no influence on the amplitude control and, furthermore, that the oscillations have settled at their final amplitude. Barkhausen's requirement expressed through Eqs.(7) to (9) is

$$\boldsymbol{A} \;=\; G_m \boldsymbol{R}_p \;=\; -1/N\,. \tag{21}$$

Invoking this condition, and using the b-function from Eq.(6), the noise voltage transfer function becomes

$$\frac{V_{n,out}(\omega)}{V_{n,in}(\omega)} \;=\; \frac{\boldsymbol{A}}{1-\boldsymbol{b}(\omega)\boldsymbol{A}} \;=\; \frac{-1/N}{1-\dfrac{1}{1+\boldsymbol{j}Q_l\beta(\omega)}} \;=\; \frac{-1}{N}\left\{1+\frac{1}{\boldsymbol{j}Q_l\beta(\omega)}\right\}, \tag{22}$$

where the frequency dependency is kept in $\beta(\omega)$. Going to noise spectra, the power spectral densities at the input and output of the oscillator, when normalized with respect to the same impedance levels, are related by the absolute square of the voltage transfer function. If $S_{n,in}(\omega)$ is the input noise spectrum and $S_{n,out}(\omega)$ the corresponding output spectrum, we have

$$\frac{S_{n,out}(\omega)}{S_{n,in}(\omega)} \;=\; \left|\frac{V_{n,out}}{V_{n,in}}\right|^2 \;=\; \frac{1}{N^2}\left\{1+\frac{1}{Q_l^2\beta^2(\omega)}\right\}. \tag{23}$$

Around the resonance frequency ω_0 we may replace the $Q_l\beta$ product by its narrowband approximation, which was introduced in section II-3. Thereby, we get expressions for the spectra in terms of the frequency deviation $\Delta\omega$ from resonance,

$$\frac{S_{n,out}(\Delta\omega)}{S_{n,in}(\Delta\omega)} \;=\; \frac{1}{N^2}\left[1+\left(\frac{\frac{1}{2}W_{3dB}}{\Delta\omega}\right)^2\right], \qquad \textit{where} \quad \begin{cases} \Delta\omega = \omega - \omega_0\,, \\ W_{3dB} = \omega_0/Q_l\,. \end{cases} \tag{24}$$

Here W_{3dB} is the usual 3dB bandwidth of the resonance circuit. We compare to only half of that because the bandwidth is defined as the distance between the 3dB point above and below

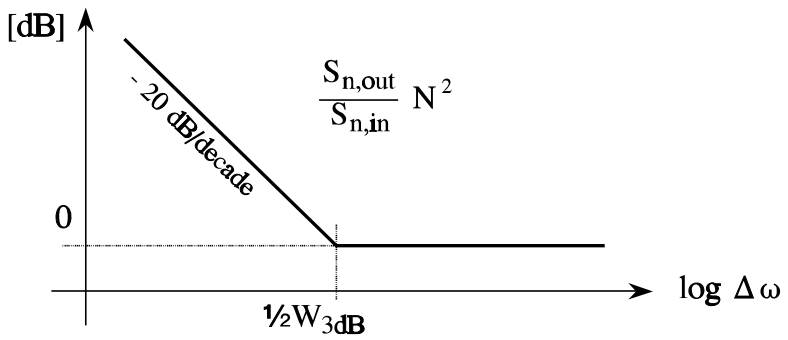

Fig.12 Asymptotic transfer characteristic between input and output noise spectra in the oscillator block-scheme from Fig.11.

ω_0 with $\Delta\omega$ being either positive or negative. A break-point characteristic corresponding to the transfer function is shown in Fig.12. It goes towards infinity when the frequency is approaching the oscillator frequency but this was expectable as Barkhausen´s condition implies infinite gain at resonance frequency if the oscillator is considered as an feedback amplifier.

Oscillators noise is commonly separated into amplitude noise, $v_{na}(t)$, and phase noise $\phi_n(t)$. The total oscillator output voltage is expressed

$$\begin{aligned} V_{out} &= \left[V_o + v_{na}(t) \right] \cos\left(\omega_0 t + \varphi_n(t)\right) \\ &= V_o \cos\omega_0 t \cos\varphi_n(t) + v_{na}(t)\cos\omega_o t \cos\varphi_n(t) \\ &\qquad V_o \sin\omega_0 t \sin\varphi_n(t) - v_{na}(t)\sin\omega_0 t \sin\varphi_n(t) \\ &\underset{|\varphi|<1}{\approx} V_o \cos\omega_0 t + v_{na}(t)\cos\omega_0 t - V_0\,\varphi_n(t)\sin\omega_0 t \ . \end{aligned} \tag{25}$$

The last approximation assumes a phase-noise much smaller than one radian, so its cosine function approximates one and the sine function approximate the phase-noise itself. Compared with an additive noise description

$$V_{out} = V_o \cos\omega_0 t + V_{n,out}(t) \ , \tag{26}$$

it is seen, that the last line in Eq.(25) is equivalent to an in-phase and quadrature resolution of the additive noise around the oscillator frequency. Starting from common additive gaussian noise sources, the noise power divides evenly between the in-phase and the quadrature terms in such a resolution. Dealing with oscillator noise, it is custom to disregard the amplitude term since the oscillator circuit is designed to keep the amplitude constant and, furthermore, the output commonly undergoes further limiting before it is applied in critical application. We shall follow this simplifying approach below.

Suppose the noise in the oscillator amplifier is white thermal noise. In equivalency to small-signal two-port noise characterization, the portion of the input noise spectrum that accounts for phase noise may be written in the form

$$S_{n,in}(\Delta\omega) = \frac{1}{2} F_{eff} N^2 k T \left[\frac{W}{Hz}\right] , \tag{27}$$

where F_{eff} is an effective noise figure that describes the amplifier under large signal sinusoidal excitation, k is Boltzman's constant, and T_o is the reference temperature for noise in Kelvin. Since this spectrum is flat, the result is directly transferred to the so-called single-sideband phase noise spectrum $\mathcal{L}(\Delta f)$. It is a spectrum like Fig.10, which is read directly from a spectrum analyzer using 1Hz resolution bandwidth. It gives the power spectral density relative to the sinusoidal output power P_o, which is proportional to $\frac{1}{2}V_o^2$. Δf denotes the difference in frequency from the oscillator signal. The simple noise model assumes a spectrum that is symmetric around the oscillator frequency. To fully include the power in one hertz bandwidth

at frequency distance |Δf| from the oscillator frequency we must include twice the value of $\mathcal{L}(\Delta f)$, where

$$\mathcal{L}_{n,out}(\Delta f) = \frac{F_{eff} k T}{2 P_o} \left\{ 1 + \left(\frac{\frac{1}{2} BW_{3dB}}{\Delta f} \right)^2 \right\} \left[Hz^{-1} \right] \tag{28}$$

In dB scale, 10 log $\mathcal{L}(\Delta f)$ is referred to as dBc, decibels over carrier. Clearly this spectrum is a scaled version of the transfer characteristic from Eq.(24) since the input spectrum is flat. However, it was discussed in the flicker noise paragraph of section IV-1, Eq.IV(21), that the 1/f noise in electron devices are transferred to the frequency range around a large sinusoidal driving signal. We have the same driving situation by the last term in Eq.(25), so including flicker noise, the input spectrum gets a 1/f term and the output may be written,

$$\mathcal{L}_{n,out}(\Delta f) = \frac{F_{eff} k T}{2 P_o} \left\{ 1 + \frac{f_a}{\Delta f} \right\} \left\{ 1 + \left(\frac{\frac{1}{2} BW_{3dB}}{\Delta f} \right)^2 \right\} \left[Hz^{-1} \right] . \tag{29}$$

where the characteristic frequency f_a is a flicker noise parameter. The expression is the final form of the Leeson oscillator model, which gets two asymptotic appearances dependent on whether f_a is smaller or larger than half the 3dB bandwidth of the resonance circuit in the oscillator. These two cases are summarized in Fig.13 (a) and (b) respectively.

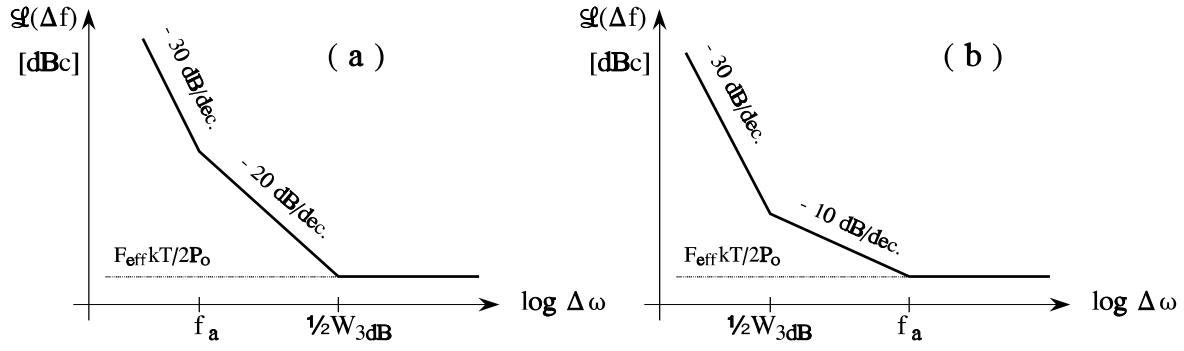

Fig.13 Asymptotic single sideband oscillator noise characteristics where in (a) resonator half-bandwidth exceeds the flicker noise bandwidth and vice versa in (b).

VI-2 Oscillator Circuits

The number of oscillator circuits that are used in practice is overwhelming, and it is impossible here to give a broad coverage. Therefore, the treatments below serves the purposes of both presenting a few common oscillator configurations and of presenting analytical techniques that also may be useful with other oscillator circuits. Furthermore, we shall point out a few important design aspects.

LC Oscillators

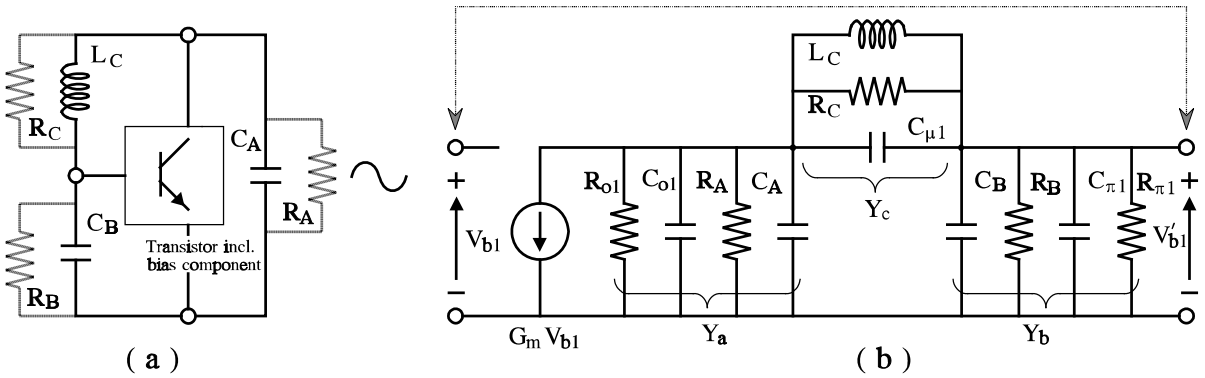

Fig.14 LC oscillator example. The equivalent circuit in (b) includes the large signal transistor model in Fig.15. Resistors R_A, R_B, and R_C may represent losses and/or loads.

Circuits intended for sinusoidal outputs up to a few GHz in frequency may be build using inductors and capacitors as tuning elements - the so called LC-oscillators. Compared with the prototype circuits in the forgoing section, the circuits we consider here are simpler in the sense that the required feed-back is inherent in the circuit topology. However, the requirements for oscillations are not identified as easily as it could be done in the transformer feed-back circuits.

One family of practical oscillator circuits, which we shall call the Colpit's family, is based on the circuit topology in Fig.14(a), where capacitors C_A, C_B, and inductor L_C are

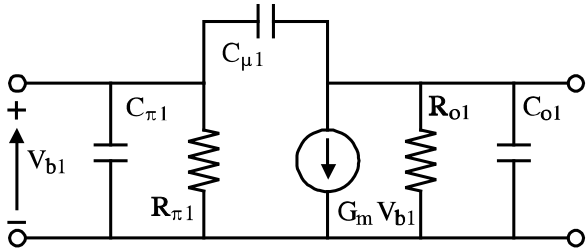

Fig.15 Transistor equivalent circuit. Under large signal conditions, the components apply to the fundamental frequency and they depend on the signal levels at the input and output ports.

supposed to be the dominant tuning elements. The transistor symbol in the diagram represents the transistor including biasing arrangements under large signal operation. At this level of approximation the transistor may be either bipolar or FET types. In the foregoing analysis of the prototype oscillator we used the simple, ohmic large signal transistor model in Fig.3(c). With caution, this model may be extended to incorporate capacitive effects, so the transistor is described by the large signal model in Fig.15. Like the simpler model, the new components $C_{\pi 1}$, $C_{\mu 1}$, C_{o1}, and R_{o1} apply to the fundamental frequency and depend on the voltages across the transistor, so the quantities are not deductible in details from the small-signal data that commonly are provided in data-sheets. However, it is seen in the equivalent circuit of Fig.14(b), which is cast in a form that facilitates open loop gain calculations, that all elements in the transistor are shunted by external components. Resistors R_A, R_B, and R_C might represent possible capacitor and inductor losses, external loads, or both. External components are expected to play the dominant role, since it is a common design objective to keep the oscillator insensitive to transistor parameter variations. For that purpose even crude approximations to the large signal transistor parameters suffices. Note finally that with exception of possible biasing contributions we may often disregard the transistor resistors $R_{\pi 1}$ in FET and R_{o1} in bipolar transistor calculations.

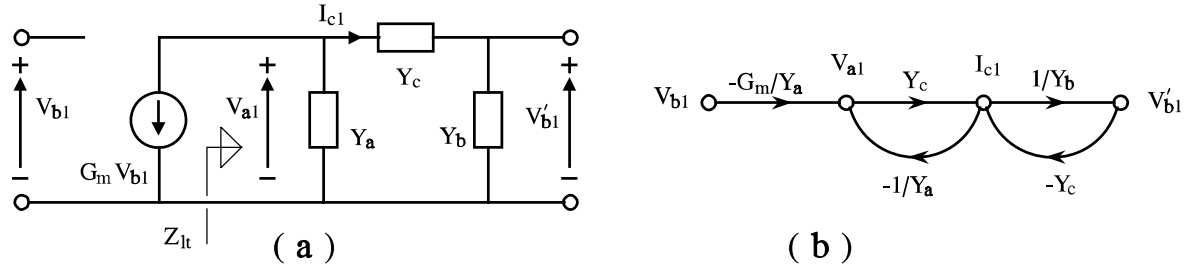

Fig.16 Circuit structure and signal flow-graph for calculating the open loop gain in the oscillator equivalent circuit from Fig.14(b).

Like the previous oscillator prototype analysis, the condition for oscillation is that the open loop gain in the circuit equals one in size and zero in phase. The structure of the circuit in Fig.14(b) has a form that is given by Fig.16. In general terms the open loop voltage gain, A_{ol} , and the criterion for oscillation are expressed,

$$A_{ol} \equiv \frac{V_{b1}^{'}}{V_{b1}} = \frac{(-G_m/Y_a)\ Y_c / Y_b}{1 + Y_c/Y_a + Y_c/Y_b} = \frac{-G_m Y_c}{Y_a Y_b + Y_c(\ Y_a + Y_b\ )}\ , \tag{30}$$

$$A_{ol} = 1 \quad \Rightarrow \quad -G_m Y_c = Y_a Y_b + Y_c\left(Y_a + Y_b\right)\ . \tag{31}$$

Inserting components

$$Y_a = g_a + jb_a\ , \qquad Y_b = g_b + jb_b\ , \qquad Y_c = g_c + jb_c\ , \tag{32}$$

and taking real and imaginary parts in Eq.(31), the condition splits into the following two conditions that must be simultaneously met,

real part condition :

$$-G_m g_c = g_a g_b - b_a b_b + g_c(g_a + g_b) - b_c(b_a + b_b) , \tag{33}$$

imaginary part condition :

$$-G_m b_c = b_a g_b + b_b g_a + b_c(g_a + g_b) + g_c(b_a + b_b) . \tag{34}$$

In details, the admittances to be inserted in the two requests are

$$g_a = 1/R_{o1} + 1/R_A , \qquad b_a = \omega_0 C_a = \omega_0 C_{o1} + \omega_0 C_A , \qquad (a)$$

$$g_b = 1/R_{\pi 1} + 1/R_B , \qquad b_b = \omega_0 C_b = \omega_0 C_{\pi 1} + \omega_0 C_B , \qquad (b) \tag{35}$$

$$g_c = 1/R_C , \qquad b_c = -1/\omega_0 L_C + \omega_0 C_{\mu 1} . \qquad (c)$$

Inserting these expressions, the two requests constitutes a system of equations that determines the frequency of oscillation ω_0 and the large signal transconductance G_m, which is necessary to maintain oscillations. Besides these two significant quantities, we shall often require the Q-factor - the loaded Q - of the open-loop gain since it determines the important properties of frequency stability and noise in the oscillator. A direct way of conducting the calculation is to find the derivative of phase with respect to angular frequency in loop gain and then, cf.Eq.(20), get the Q-factor from the relationship

$$Q_l = \frac{\omega_0}{2} \left| \frac{d \angle A_{ol}}{d\omega} \right|_{\omega_0} . \tag{36}$$

Finally, the loading of the transistor might be required to check whether or not a device is adequate in a given application. According to Fig.16 and Eq.(30), the load impedance seen from the port of the tranconductance current generator is given through

$$\frac{V_{a1}}{V_{b1}} = \frac{-G_m/Y_a(1 + Y_c/Y_b)}{1 + Y_c/Y_a + Y_c/Y_b} = \frac{V_{b1}'}{V_{b1}} \left(\frac{Y_b}{Y_c} + 1 \right) \underset{\text{osc. criterion}}{=} \left(\frac{Y_b}{Y_c} + 1 \right) \Rightarrow \tag{37}$$

$$Z_{lt} = \frac{V_{a1}}{-G_m V_{b1}} = \frac{-1}{G_m} \left(\frac{Y_b}{Y_c} + 1 \right) . \tag{38}$$

The oscillator circuit topology in Fig.14(a) contains no ground node and the corresponding criteria for oscillations are independent of which one of the transistor terminal that is set to - or taken as - the signal ground. Distinctions between the different ways of grounding is made from practical reasons since the literature often refer to circuits named after their

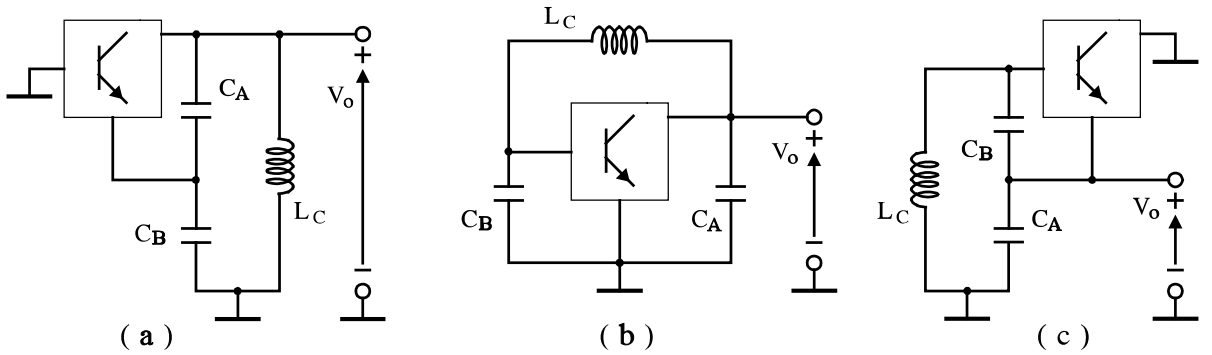

Fig.17 Colpitt's (a), Pierce (b), and Seiler (c) oscillators. They are deduced from Fig.14 by grounding base, emitter, or collector - gate, source, or drain - respectively.

inventors. The tree possibilities with the present topology are summarized in Fig.17. They are known as Colpitts, Pierce and Seiler oscillators. Considering the figures it should still be kept in mind that the transistor symbol represents a transistor under large signal operation, either bipolar's or FET's. It includes the type of bias network that is required to reduce transconductance and in turn stabilize the oscillation amplitude. Note also that the output indications in the figures are suggestions as any non-grounded node in the circuit has an oscillating voltage component. Which one to use depends on the application since the different nodes differ with respect to distortion, noise, and output power capabilities if they are loaded.

Simplified Analysis of Colpitts Family of Oscillators

To illuminate and to make practical use of the conditions from Eqs.(33) to (38), we consider a few simplified situations where it is assumed that the transistor feed-back capacitance is negligible, so the susceptances are in all cases given by

$$\begin{aligned} b_a &= \omega_0 C_a = \omega_0 (C_A + C_{o1}), && (a) \\ b_b &= \omega_0 C_b = \omega_0 (C_B + C_{\pi 1}), && (b) \\ b_c &= -1 / \omega_0 L_C . && (c) \end{aligned} \tag{39}$$

Assume for a moment that there were no resistive losses in the circuit, i.e.

$$g_a = g_b = g_c = 0. \tag{40}$$

In this hypothetical situation, the real part condition from Eq.(33) provides

$$\begin{aligned} 0 = -\omega_0^2 C_a C_b + \frac{C_a + C_b}{L_C} \quad \Rightarrow \quad \omega_0 = \omega_{00} \quad \textit{where} \\ \omega_{00}^2 \equiv \frac{C_a + C_b}{L_C C_a C_b} = \frac{1}{L_C C_{ser}}, \quad C_{ser} = \frac{C_a C_b}{C_a + C_b} . \end{aligned} \tag{41}$$

As seen, the frequency of oscillation ω_0 becomes the resonance frequency ω_{00} of an ideal resonance circuit made of inductor L_C and the series connection of capacitances C_a and C_b. The corresponding imaginary part condition implies

$$G_m / \omega_0 L_C = 0 \quad \Rightarrow \quad G_m = 0, \tag{42}$$

which means that once the oscillations have started, there are no need for an active element to compensate resistive losses, since they are absent in this particular case. Below we shall include losses and find the corresponding transconductance requirements. Since the analysis becomes involved with more than one resistive component, we assume one dominant resistive component in the initial calculations. Afterwards, the results may be slightly adjusted to correct for less significant losses.

Case 1 in load resistor placement

If the only ohmic component resides across the transistor output terminals the equivalent diagram becomes the one shown in Fig.18. The conductances are

$$g_a = \frac{1}{R_a} = \frac{R_A + R_{o1}}{R_A R_{o1}}, \qquad g_b = g_c = 0. \tag{43}$$

The real-part condition and, consequently, the frequency of oscillation remains unaltered from the results in Eq.(41). The imaginary part condition now provides

$$\frac{G_m}{\omega_0 L_C} = \frac{\omega_0 C_b}{R_a} - \frac{1}{\omega_0 L_C R_a} \quad \Rightarrow \quad G_m = \frac{1}{R_a}\left[\omega_0^2 L_C C_b - 1\right]. \tag{44}$$

i.e. is an expression for the size of the transconductance that the transistor must approach when oscillations build up to the desired amplitude. Including the oscillation frequency from Eq.(41), we get

$$G_m = \frac{1}{R_a}\left[\frac{C_a + C_b}{C_a} - 1\right] = \frac{1}{R_a}\frac{C_b}{C_a}. \tag{45}$$

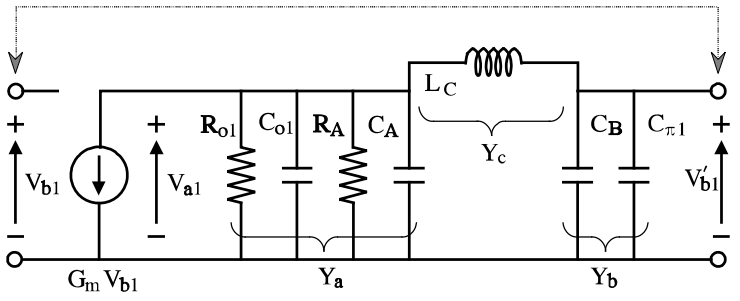

Fig.18 Equivalent circuit for the oscillator loop gain with simplifying assumptions, no transistor feed-back and resistive loading across the transistor output terminals only.

To find the Q-factor of the open-loop gain, direct insertion of Eq.(43) into Eq.(30) gives

$$A_{ol}(j\omega) = \frac{-G_m / j\omega L_C}{j\omega C_b (1/R_a + j\omega C_a) + (1/R_a + j\omega (C_a + C_b))/\omega L_C} = \frac{-G_m}{(1-\omega^2 L_C C_b)/R_a + j\omega (C_b + C_a(1-\omega^2 L_C C_b))} \quad \Rightarrow \tag{46}$$

$$\angle A_{ol} = -\tan^{-1}\left\{ R_a \omega \left[\frac{C_b}{1-\omega^2 L_C C_b} + C_a \right] \right\} . \tag{47}$$

At the oscillation frequency $\omega=\omega_0$ this angle should vanish and direct substitution from Eq.(41) reveals that the expression in brackets becomes zero. The derivative with respect to angular frequency at ω_0 now develops

$$d\tan^{-1} x = \frac{1}{1+x^2} dx, \quad where \quad \omega = \omega_0 \sim x = 0 \quad \Rightarrow$$
$$\left. \frac{d\angle A_{ol}}{d\omega} \right|_{\omega_0} = -R_a \omega_0 C_b \frac{2\omega_0 L_C C_b}{\left(1-\omega_0^2 L_C C_b\right)^2} = -2R_a (C_a + C_b) \frac{C_a}{C_b} , \tag{48}$$

and the corresponding Q-factor becomes

$$Q_l = \frac{\omega_0}{2} \left| \frac{d\angle A_{ol}}{d\omega} \right|_{\omega_0} = R_a \omega_0 (C_a + C_b) \frac{C_a}{C_b} . \tag{49}$$

Here we have demonstrated a direct approach to the Q-factor calculation. It may seem cumbersome, but it has the virtue that we don't need to identify and refer all ohmic losses to a particular resonance circuit. In the present simplified case with only one resistor we may, however, easily check the result as we have already seen, that the oscillating frequency is set

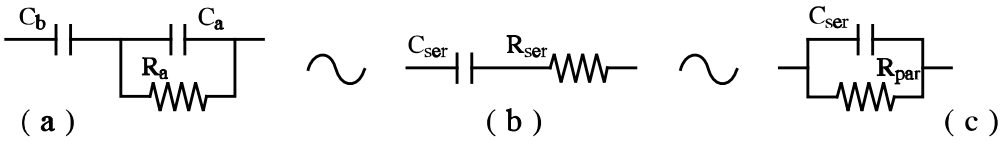

Fig.19 Parallel to series to parallel conversion used for estimating the Q-factor in the oscillator from Fig.18.

by resonance between inductor L_C and the series connection of C_a and C_b. Since R_a appear across C_a, its equivalent series resistance R_{ser} in Fig.19(b) is determined by this capacitor, but it is also the total series loss in resonance with the series connected capacitors. By parallel-to-series transformations according to Eq.(III-59), we get

$$R_{ser} = \frac{1}{\omega_0^2 C_a^2 R_a} \quad \Rightarrow$$
$$Q_l = \frac{1}{\omega_0 C_{ser}} \frac{1}{R_{ser}} = \frac{C_a + C_b}{\omega_0 C_a C_b} \omega_0^2 C_a^2 R_a = R_a \omega_0 (C_a + C_b) \frac{C_a}{C_b} . \tag{50}$$

i.e. the same result as before. Clearly we would also get this result - which is included here for future reference - by transforming to parallel form like Fig.19(c), where

$$R_{par} = \frac{1}{\omega_0^2 C_{ser}^2 R_{ser}} = \left(\frac{C_a + C_b}{C_b} \right)^2 R_a \Rightarrow$$
$$Q_l = \omega_0 C_{ser} R_{par} = \omega_0 \frac{C_a C_b}{C_a + C_b} \frac{(C_a + C_b)^2 R_a}{C_b^2} = R_a \omega_0 (C_a + C_b) \frac{C_a}{C_b} . \tag{51}$$

The voltage gain around the transistor and the transistor load are calculated by Eqs.(37), (38), and (45) to yield

$$\frac{V_{a1}}{V_{b1}} = \frac{Y_b}{Y_c} + 1 = -\omega_0^2 L_C C_b + 1 = -\frac{C_b}{C_a} , \qquad Z_{lt} = \frac{-1}{G_m} \frac{V_{a1}}{V_{b1}} = R_a . \tag{52}$$

Case 2 in load resistor placement

The second simplified case we consider has resistive loading across the transistor input terminalsas seen in Fig.20. Here the simplified analysis is based on the conductances,

$$g_a = 0 , \qquad g_b = \frac{1}{R_b} = \frac{R_{\pi 1} + R_B}{R_{\pi 1} R_B} , \qquad g_c = 0 . \tag{53}$$

Again, the real-part condition and the frequency of oscillation remain unaltered from the results in Eq.(41). The imaginary part condition provides

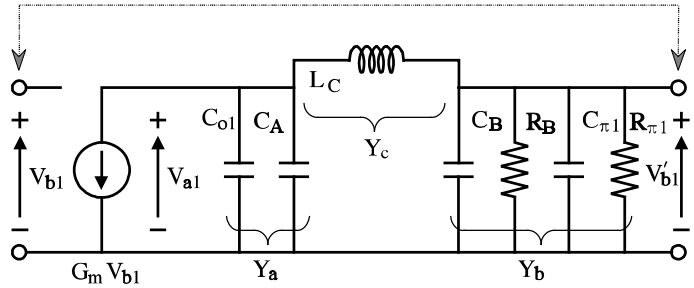

Fig.20 Equivalent circuit for the oscillator loop gain with simplifying assumptions, no transistor feed-back and resistive loading across the transistor input terminals only.

$$\frac{G_m}{\omega_0 L_C} = \frac{\omega_0 C_a}{R_b} - \frac{1}{\omega_0 L_C R_b} \quad \Rightarrow \quad G_m = \frac{1}{R_b}\left[\omega_0^2 L_C C_a - 1\right] = \frac{1}{R_b}\frac{C_a}{C_b}. \tag{54}$$

Compared with Fig.19(a), a-terms and b-terms have changed roles, so in analogy to Eq.(50), the Q-factor with resistive losses across the transistor input port becomes

$$Q_l = \frac{1}{\omega_0 C_{ser}}\frac{1}{R_{ser}} = \frac{C_a + C_b}{\omega_0 C_a C_b}\,\omega_0^2 C_b^2 R_b = R_b\,\omega_0(C_a + C_b)\frac{C_b}{C_a}. \tag{55}$$

Finally, the voltage gain and the load at the frequency of oscillation from Eqs.(37) and (38) simplify to

$$\frac{V_{al}}{V_{bl}} = \frac{j\omega_0 C_b + 1/R_b}{1/j\omega_0 L_C} + 1 = -\frac{C_b}{C_a} + j\,\frac{\omega_0 L_C}{R_b} \tag{56}$$

$$Z_{tr} = \frac{-1}{G_m}\frac{V_{al}}{V_{bl}} = R_b\left(\frac{C_b}{C_a}\right)^2 - j\,\omega_0 L_C\frac{C_b}{C_a}. \tag{57}$$

In contrast to the previous case, gain and load impedance now get small imaginary components as a consequence of the reactive separation between the transistor transconductance and the ohmic load. However, the higher R_b, the higher Q, and the less significant become the imaginary components.

Case 3 in load resistor placement

The final simplified case to consider is the one where the load and losses connect across the inductance L_C as indicated by Fig.21. There are no components from the transistor equivalent circuit in this position, so the conductances are given by

$$g_a = g_b = 0, \qquad g_c = \frac{1}{R_C}. \tag{58}$$

In this case, the real part and the imaginary part conditions from Eqs.(33) and (34) are no longer independent, since

$$\begin{aligned} \textit{real part condition}: \quad & -\frac{G_m}{R_c} = -\omega_0^2 C_a C_b + \frac{C_a + C_b}{L_C}, \\ \textit{imaginary part condition}: \quad & \frac{G_m}{\omega_0 L_C} = \frac{\omega_0(C_a + C_b)}{R_C}. \end{aligned} \tag{59}$$

The last equation is similar to

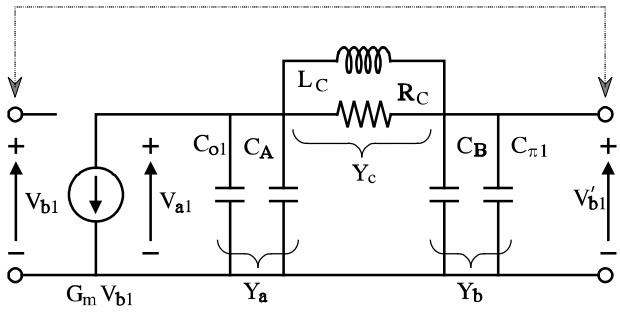

Fig.21 Equivalent circuit for the oscillator loop gain with simplifying assumptions, no transistor feed-back and resistive loading across the inductor only.

$$\frac{G_m}{R_C} = \frac{\omega_0^2 L_C (C_a + C_b)}{R_C^2} . \tag{60}$$

which - when inserted in the real part condition - provides

$$\omega_0^2 \left[C_a C_b - \frac{L_C (C_a + C_b)}{R_C^2} \right] = \frac{C_a + C_b}{L_C} \quad \Rightarrow \quad \omega_0^2 = \omega_{00}^2 \left[1 + \frac{1}{Q_L^2 - 1} \right] , \tag{61}$$

Here we have used the resonance frequency ω_{00} defined in Eq.(41) and the quality factor Q_L for the inductor at resonance ,

$$Q_L \equiv \frac{R_C}{\omega_{00} L_C} . \tag{62}$$

It is seen that the larger Q_L, the closer comes the oscillator frequency to the resonance frequency ω_{00}. Since the only resistive loss is provided by R_C, the inductor Q-factor Q_L becomes also the Q-factor for the oscillator. Inserting the oscillator frequency into Eq.(60) gives the necessary transconductance,

$$G_m = \frac{\omega_{00}^2 L_C (C_a + C_b)}{R_C} \left[1 + \frac{1}{Q_L^2 - 1} \right] \underset{Q_L \gg 1}{\approx} \frac{1}{R_C} \frac{(C_a + C_b)^2}{C_a C_b} . \tag{63}$$

The voltage gain and the transistor load become

$$\frac{V_{a1}}{V_{b1}} = \frac{j \omega_0 C_b}{1/j \omega_0 L_C + 1/R_C} + 1 \approx \frac{- \omega_0^2 L_C C_b}{1 + j/Q_L} + 1 \approx - \frac{C_b}{C_a} , \tag{64}$$

$$Z_{tr} = \frac{-1}{G_m} \frac{V_{a1}}{V_{b1}} = R_C \left(\frac{C_b}{C_a + C_b} \right)^2 . \tag{65}$$

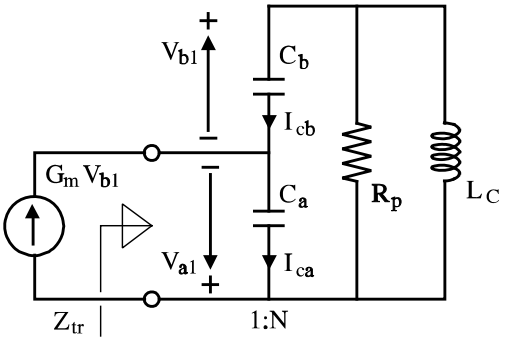

Fig.22 Oscillator equivalent circuit. Parallel resistance R_p accounts for all resistive losses in the circuit.

Arbitrary resistor placements

A unified approach to the three cases above can be achieved through Fig.22, where resonance circuit and capacitive transformer properties of the oscillator are emphasized. The transformation ratio is, cf. sec.II-6,

$$N = \frac{C_a + C_b}{C_b} , \tag{66}$$

With high Q-factors, the reactive currents in L_C and the series connection of C_a and C_b at resonance are large compared to the loss currents through R_p or, equivalently the transistor load, Z_{tr0}, which may be expressed

$$Z_{tr} = Z_{tr0} = \frac{R_p}{N^2} = R_p \frac{C_b^2}{(C_a + C_b)^2} . \tag{67}$$

Accordingly, the capacitive current I_{ca} is nearly equal to I_{cb}, and the voltage ratio across the two capacitors becomes inversely proportional to the capacitances,

$$\frac{V_{bl}}{V_{al}} \approx - \frac{C_a}{C_b} \qquad \left(= 1 - N \right) . \tag{68}$$

To maintain oscillations the loop gain must be one so voltage V_{b1} across C_{b1} in the diagram equals the control voltage for transconductance G_m. We get

$$G_m Z_{tr0} \frac{V_{bl}}{V_{al}} = 1 \qquad \Rightarrow \qquad G_m = \frac{1}{R_p} \frac{(C_a + C_b)^2}{C_a C_B} \tag{69}$$

where the last expression sets the requirement to G_m. With R_p set to R_C it is seen that the G_m we have just derived corresponds to the value in Eq.(63) as expected, since the diagram in Fig.22 is a reorganization of the diagram in Fig.21. More noticeably is the observation that

if we replace R_p with the equivalent parallel resistor R_{par} from Eq.(51) for losses that are concentrated across the transistor output port, we get

$$G_m = \frac{1}{R_{par}} \frac{(C_a + C_b)^2}{C_a C_b} = \frac{1}{R_a} \frac{C_b}{C_a} . \tag{70}$$

which is the same as the G_m request in Eq.(45). Had we made a similar derivation from Eq.(69) in the case where ohmic losses are concentrated across the transistor input terminal like in Fig.20, we would have obtained the transconductance value in Eq.(54). Thus we estimate G_m correctly from different loss components taken one by one if they are transformed to the parallel equivalent resistance R_{par}. This fact suggests that the joint effect upon G_m of more losses from different locations in the circuit may be calculated from a parallel connection of their equivalent parallel resistances. We may even use series-to-parallel transformation to convert all loss contributions to one of the special case that were considered if it suits our need for making other design calculation. Such approaches are much simpler than an attempt to solve the corresponding real and imaginary part condition simultaneously. We shall demonstrate them in the following two examples.

Example VI-2-1 (Seiler type LC oscillator)

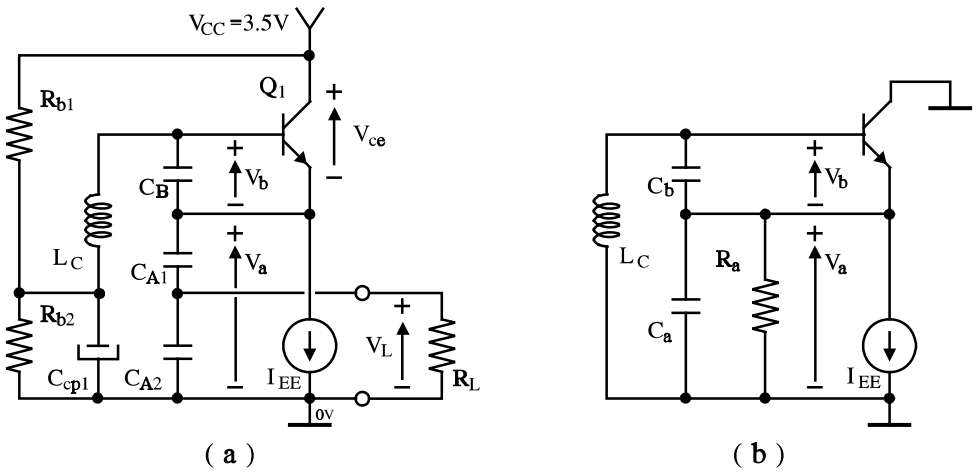

Fig.23 Seiler oscillator. With exception of current bias details, part (a) shows the circuit diagram while part (b) shows the functional diagram that is used in the design.

The oscillator circuit in Fig.23(a) is a Seiler circuit where the transistor is current biased, presently without showing details on how this is made in practice. The tuning capacitor across the transistor output port is made of a series connection, C_{A1} and C_{A2}, which transforms the required load resistance R_L to a larger equivalent transistor load resistance, R_a, as indicated by the functional diagram in Fig.23(b). This way we get more suitable component values and better utilization of the battery supply than a direct connection of the load to the transistor would provide. Resistors R_{b1} and R_{b2} are base bias resistors and C_{cp1} is a decoupling capacitor. The main requirements to the circuit are

- frequency, f_0 = 300 MHz,
- output power, P_{out} = 2 mW in R_L=50Ω,
- loaded Q-factor, Q_l > 20,
- gain reduction at nominal output, G_m:g_m ~ 1:2.5

It is furthermore assumed that the transistor requires $V_{ce} > V_{ce,min}$=0.5V to prevent saturation effects and that it has a forward current gain $\beta_f = 50$, equivalently $\alpha_f = 0.98$.

We shall assume that the load R_a is the only resistive component in the oscillator equivalent circuit, so the design corresponds to the first case that was considered above in conjunction with the equivalent circuit in Fig.18. To find the equivalent load resistor R_a assume that the transistor output voltage swing V_{a1} is half the battery voltage minus two times the minimum voltage $V_{ce,min}$, where the first count comes from transistor Q_1, the second count leaves room for a transistor in the bias current generator. With V_{a1} fixed, the corresponding load resistor is calculated from the output power requirement,

$$V_{a1} = \frac{1}{2}\left(V_{CC} - 2V_{ce,\min} \right) = \frac{1}{2}(3.5 - 1.) = 1.25[V], \tag{71}$$

$$P_{out} = \frac{V_a^2}{2R_a} \quad \Rightarrow \quad R_a = \frac{V_{a1}^2}{2P_{out}} = \frac{1.25^2}{2 \cdot 2 \cdot 10^{-3}} = 390.6[\Omega]. \tag{72}$$

According to Eq.(5-100) and Figure 5-44 in chapter 5, a 1:2.5 reduction in gain when the oscillations grow up requires the final drive level x_{max}, which is normalized with respect to the thermal voltage V_t=kT/q~25mV, where

$$x = x_{max} = 4.3 = \left| \frac{V_{b1}}{V_t} \right| \quad \Rightarrow \quad V_{b1} = 4.3 \cdot 0.025 = 0.1075[V]. \tag{73}$$

To find the capacitances C_a and C_b, Eqs.(50) and (52) provide

$$\frac{C_b}{C_a} = \left| \frac{V_{a1}}{V_{b1}} \right| = \frac{1.25}{0.1075} = 11.63, \tag{74}$$

$$R_a \omega_0 (C_a + C_b) \frac{C_a}{C_b} = Q_{lmin} = 20 \quad \Rightarrow$$

$$C_a + C_b = \frac{Q_{lmin}}{R_a \omega_0} \frac{C_b}{C_a} = \frac{20 \cdot 11.63}{390.6 \cdot 2\pi\, 300 \cdot 10^6} = 315.9 \cdot 10^{-12} \tag{75}$$

$$C_b = \frac{C_a + C_b}{1 + C_a/C_b} = \frac{315.9 \cdot 10^{-12}}{1 + 1/11.63} = 290.9[pF], \quad C_a = \frac{C_b}{11.63} = 25.01[pF].$$

The tuning condition follows from Eq.(41), which gives

$$C_{ser} = \frac{C_a C_b}{C_a + C_b} = \frac{25.01 \cdot 290.9}{315.9} = 23.03\,[pF] \quad \Rightarrow$$
$$L_C = \frac{1}{\omega_0^2 C_{ser}} = \frac{1}{(2\,\pi\,300 \cdot 10^6)^2\, 23.03 \cdot 10^{-12}} = 12.22 \cdot 10^{-9} \sim 12.22\,[nH]\ . \tag{76}$$

Impedance transformation from R_L to R_a implies the transformation ratio

$$N^2 = \frac{R_a}{R_l} \quad \Rightarrow \quad N = \frac{C_{A1} + C_{A2}}{C_{A1}} = \sqrt{\frac{R_a}{R_L}} = \sqrt{\frac{390.6}{50}} = 2.795\ , \tag{77}$$

so the two capacitances that connect to C_a become

$$C_a = \frac{C_{A1} C_{A2}}{C_{A1} + C_{A2}} = \frac{C_{A2}}{N} \quad \Rightarrow \quad \begin{cases} C_{A2} = C_a N = 25.01 \cdot 2.795 = 69.90\,[pF]\ , \\ C_{A1} = \dfrac{C_{A2}}{N-1} = \dfrac{69.90}{1.796} = 38.92\,[pF]. \end{cases} \tag{78}$$

To keep the oscillations running, the final large signal conductance is given by Eq.(45),

$$G_m = \frac{1}{R_a}\,\frac{C_b}{C_a} = \frac{11.63}{390.6} = 0.0298\,[S]\ . \tag{79}$$

The DC bias current I_{EE} is now calculated from the current gain reduction of 1:2.5. We get

$$g_m = \frac{\alpha_f I_{EE}}{V_t} = 2.5\,G_m \quad \Rightarrow$$
$$I_{EE} = \frac{2.5\,G_m\,V_t}{\alpha_f} = \frac{2.5 \cdot 0.0298 \cdot 0.025}{0.98} = 0.00190 \sim 1.90\,[mA]\ . \tag{80}$$

The final step in the design is to fix the base biasing and to implement the I_{EE} current source. In agreement with the initial emitter oscillator amplitude calculation in Eq.(71), the mean emitter voltage V_{e0} is given by

$$V_{e0} = V_{CC} - V_{ce,\min} - V_{a1} = 3.5 - 0.5 - 1.25 = 1.75\,[V]\ . \tag{81}$$

When oscillations grow up and the transistor is forced into class C operation, the mean base emitter voltage will be slightly reduced from its initial DC value, which commonly is in the range of V_{be0}=0.65V. We ignore this adjustment here since the effect is small with current biasing, so the base DC-bias voltage should be $V_{b0}=V_{be0}+V_{e0}$=2.4V. Choosing the common DC current I_{br} through R_{b1} and R_{b2} to be approximately ten times the base dc current, which is $I_{b0}\sim I_{EE}/\beta_f$=0.04mA, i.e. I_{br}=0.4mA, the bias resistors become

$$R_\Sigma \equiv R_{b1} + R_{b2} = \frac{V_{CC}}{I_{br}} = \frac{3.5}{0.4\cdot 10^{-3}} = 8.75\cdot 10^3 \Rightarrow \tag{82}$$

$$R_{b2} = \frac{V_{b0}}{V_{cc}} R_\Sigma = \frac{2.40}{3.5} 8.75\cdot 10^3 = 6.00[k\Omega], \quad R_{b1} = R_\Sigma - R_{b2} = 8.75 - 6.00 = 2.75[k\Omega].$$

The decoupling capacitor C_{cp1} should be chosen so its reactance at the oscillation frequency is small compared to both the parallel connection of R_{b1} and R_{b2} and to the reactance of L_C. The last requirement is the strongest since $R_{b1}\|R_{b2}$~1.9kΩ while $\omega_0 L_C = R_a/Q = 20\Omega$. Following the results from Eq.(76), we chose

$$\frac{1}{\omega_0 C_{cp1}} \ll \omega_0 L_C \quad \Rightarrow \quad C_{cp1} \gg \frac{1}{\omega_0^2 L_C} = C_{ser} = 23.03[pF]: \qquad C_{cp1} = 2.0[nF]. \tag{83}$$

Current biasing may ideally be implemented by a current mirror as sketched in Fig.24(a). If transistors Q_2 and Q_3 are identical, R_{b3} should be adjusted so that its current equals the bias current I_{EE}. Less ideally, current biasing may be provided simply by a large resistor as show in Fig.24(b). With the DC currents and voltages from above, the resister should be

$$R_{EE} = \frac{V_{e0}}{I_{EE}} = \frac{1.75}{1.90\cdot 10^{-3}} = 921[\Omega]\ . \tag{84}$$

Although this value is significantly larger than the equivalent load resistor R_a, which R_{EE} is connected across, the power loss at the oscillation frequency in R_{EE} cannot be ignored compared to the output requirement. If this simpler solution is chosen, the design should be adjusted to compensate for the additional loss.

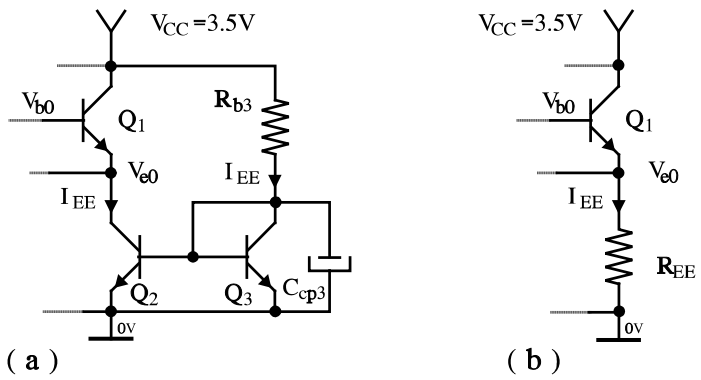

Fig.24 Current bias methods for the Seiler oscillator using, (a), a current mirror or, (b), a large resistor R_{EE}.

Example VI-2-1 end

Example VI-2-2 (Pierce type LC oscillator)

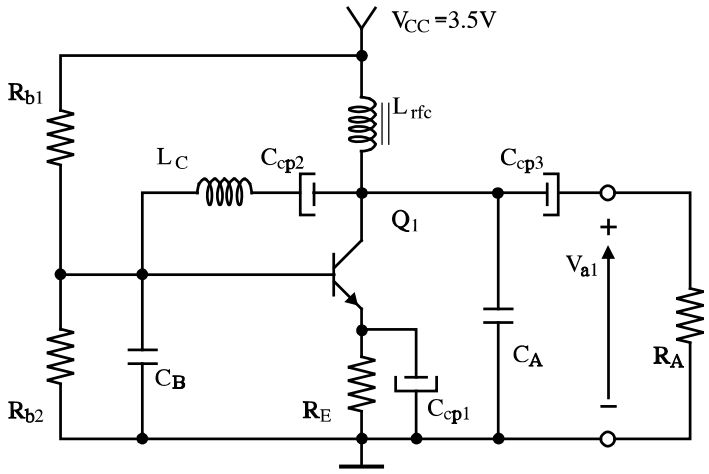

Fig.25 Pierce oscillator. The transistor is driven into class C operation to provide a self-limiting gain.

Fig.25 shows the complete diagram for a Pierce oscillator build around a bipolar transistor. The emitter is biased through R_E, capacitor C_{cp1} is a decoupling capacitor, to provide self-limiting gain. The oscillating frequency is determined by L_C, C_A, and C_B. C_{cp2}, C_{cp3} are coupling capacitors, and L_{rfc} is a RF choke, i.e. it has little DC resistance for bias but provides a large impedance at the oscillating frequency. Finally, resistors R_{b1} and R_{b2} provide the base biasing.

The Pierce oscillator above should be designed to meet the following requirements,

- frequency, f_0 = 10 MHz,
- output V_{a1}= 1.6 V_p in R_A = 600 Ω,
- 2nd and higher harmonic output components below -36dBc each,
- approximate gain reduction at nominal output G_m/g_m ~ 1:3.

Furthermore, it is assumed that inductor L_C has a Q-factor of 150 or more and that the transistor has current gain β=60 or, correspondingly, α_f=0.98. V_{ce} should be kept above $V_{ce,min}$ = .6 V to prevent distortion by saturation effects in the transistor.

We know from the forgoing chapter on nonlinear amplifiers, that the class C operated amplifier stage in Fig.25, which includes a bypassed emitter resistor, cannot be solved analytically from the set of specifications at hand. Therefore, the design strategy is to start with a few initial assumption, which must be verified in the course of the work. The first one concerns the driving level V_{b1} at the transistor input. In the limit of $R_E \rightarrow \infty$ it is seen in Figure 5-44 - using $A \rightarrow \infty$ - that a relative input level reduction of 1:3 requires a relative input level of x≈6, i.e.

$$x = 6 \quad \Rightarrow \quad V_{b1} = x V_t = 6 \cdot 25\,[mV] = 0.150\,[V] \; . \tag{85}$$

According to the discussion of the bipolar parallel tuned amplifier on page 19 in chapter 5, we see from Figure 5-16 that for a given argument x - the second order modified Bessel function is greater than third and any higher order functions. Since the harmonic components in the collector current over the fundamental frequency component is the ratio of the corresponding ordered modified Bessel function over the 1st order function, the 2nd harmonic component introduces the largest distortion and is the one to be used in the design. Using Figure 5-16 we get

$$\hat{I}_1(6) = 61\ , \quad \hat{I}_2(6) = 47 \quad \Rightarrow \quad \frac{I_{c2}}{I_{c1}} = \frac{\hat{I}_2(6)}{\hat{I}_1(6)} = \frac{47}{61} = 0.77\ . \tag{86}$$

The fundamental frequency output voltage component corresponds to resonance in the resonance circuit containing L_C and the series connection of C_a and C_b. The collector load impedance is a downscaled version of this circuit which at resonance is Z_{tr0}. The corresponding impedance at n times the resonance frequency is

$$Z_{tr,n} = Z_{tr}(n\,\omega_0) = \frac{Z_{tr0}}{1 + j\,Q_l\,(n - 1/n)}\ , \tag{87}$$

where Q_l is the total loaded Q-factor for the resonance circuit. Imposing the distortion requirements for 2nd order harmonic components, we get

$$\left|\frac{V_{a2}}{V_{a1}}\right| = \left|\frac{Z_2}{Z_1}\,\frac{I_{c2}}{I_{c1}}\right| = \frac{1}{\sqrt{1 + Q_l^2(2 - 1/2)^2}}\,\frac{\hat{I}_2(6)}{\hat{I}_1(6)} \le 0.0158 \sim -36[dB] \quad \Rightarrow \tag{88}$$

$$Q_l \ge \frac{1}{1.5}\sqrt{\left(\frac{\hat{I}_2(6)}{\hat{I}_1(6)}\,\frac{V_{a1}}{V_{a2}}\right)^2 - 1} = \frac{1}{1.5}\sqrt{(0.763/0.0158)^2 - 1} = 32.18\ .$$

This Q-factor is considerably smaller than the Q-factor that represents losses in inductor L_C, the internal losses, and load resistor R_A is supposed to contribute most significantly to the total loss in the circuit. Other contributions to the internal losses come from the transistor input impedance and biasing networks, so we design with an internal Q-factor that is somewhat lower than Q_L, say Q_{int}=120, and verify that we stay within specifications afterwards. As R_A is still the most significant loss, it is natural to use our first special case as foundation for the design, i.e. use the circuit in Fig.18 and the pertinent equations. However, we should first modify the load to a resistor R_A' that incorporates the internal losses. The latter are represented by a resistor R_{int} across R_A. Following the terminology that was introduced in section II-4, the Q-factor corresponding to R_A may be referred to as the external Q-factor, Q_{ext}. Due to the parallel connections and the proportionality between Q-factors and parallel resistors we have

$$\left.\begin{aligned} \frac{1}{Q_l} &= \frac{1}{Q_{ext}} + \frac{1}{Q_{int}} \\ \frac{1}{R_A'} &= \frac{1}{R_A} + \frac{1}{R_{int}} \end{aligned}\right\} \quad \Rightarrow \quad R_A' = R_A \left[1 - \frac{Q_l}{Q_L} \right] = 600 \left[1 - \frac{32.18}{120} \right] = 439.1\,[\Omega]. \tag{89}$$

The equivalent intrinsic loss resistance to be parallelled across R_A has the size

$$R_{int} = \frac{R_A R_A'}{R_A - R_A'} = \frac{600 \cdot 431.1}{600 - 431.1} = 15531 \sim 1.531[k\Omega] \ . \tag{90}$$

Using Eqs.(50) and (52) we get

$$\frac{C_b}{C_a} = \left| \frac{V_{a1}}{V_{b1}} \right| = \frac{1.6}{0.150} = 10.67 \ , \qquad Q_l = R_A' \omega_0 (C_a + C_b) \frac{C_a}{C_b} \qquad \Rightarrow$$

$$C_\Sigma \equiv C_a + C_b = \frac{C_b}{C_a} \frac{Q_l}{R_A' \omega_0} = \frac{10.67 \cdot 32.18}{439.1 \cdot 2\pi \cdot 10^7} = 12.45\,[nF], \tag{91}$$

$$C_a = \frac{C_\Sigma}{1 + C_b / C_a} = \frac{12.45}{11.67} = 1.066\,[nF], \quad C_b = C_\Sigma - C_a = 12.45 - 1.066 = 11.38\,[nF] \ .$$

The corresponding inductor is given by

$$C_{ser} = \frac{C_a C_b}{C_a + C_b} = \frac{1.066 \cdot 11.38}{12.45} = 0.9744\,[nF] \ , \tag{92}$$

$$L_C = \frac{1}{C_{ser}\, \omega_0^2} = \frac{1}{0.9744 \cdot 10^{-9} (2\pi 10^7)^2} = 260.0\,[nH] \ .$$

When the circuit oscillates with the assumed output voltage swing of 1.6 V_p, the corresponding fundamental frequency collector current component is

$$I_{c1} = V_{a1} / R_A' = 1.6 / 439.1 = 3.643 \cdot 10^{-3} \sim 3.643\,[mA]. \tag{93}$$

With a relative driving level of x=6, the corresponding collector and emitter DC currents with ongoing oscillations are

$$I_{c0} = \frac{\hat{I}_0(6)}{2\,\hat{I}_1(6)}\, I_{c1} = \frac{67.2}{2 \cdot 61.3}\, I_{c1} = 0.548 \cdot 3.643 = 1.997\,[mA] \ , \tag{94}$$

$$I_{e0} = I_{co} (1 + 1/\beta) = 1.997 (1 + 1/60) = 2.030\,[mA] \ .$$

The difference between the supply voltage and the DC voltage across R_E must leave room for the output swing and the minimum collector-emitter voltage. In order to meet the assumption of $R_E \to \infty$, we choose R_E as large as possible and get

$$V_{E0} = V_{CE} - V_{a1} - V_{ce,\min} = 3.5 - 1.6 - 0.6 = 1.3\,[V] \quad \Rightarrow$$
$$R_E = \frac{V_{E0}}{I_{e0}} = \frac{1.3}{2.030 \cdot 10^{-3}} = 640\,[\Omega]. \tag{95}$$

The large signal fundamental frequency transconductance and transistor input impedance become

$$G_m = \frac{1}{R_A}\frac{C_b}{C_a} = \frac{10.67}{439.1} = 24.30\,[mS], \quad R_{\pi 1} = \frac{\beta}{G_m} = \frac{60}{24.30 \cdot 10^{-3}} = 2.430\,[k\Omega]. \tag{96}$$

The gain reduction factor of three leds to the initial assumption of a nearly constant transistor bias current. We may check the assumption from the small-signal transconductance g_m, the corresponding DC-current I_{c00}, and the design constant A, which guided our decision on basis of Figure 5-44. We get

$$g_m = 3\,G_m = 3 \cdot 2.469 \cdot 10^{-3} = 72.90 \cdot 10^{-3} \quad \Rightarrow \quad A = \frac{g_m R_E}{\alpha_f} = \frac{.0729 \cdot 640}{0.98} = 47.6,$$
$$g_m = \frac{I_{c00}}{V_t} \quad \Rightarrow \quad I_{c00} = g_m V_t = 72.9 \cdot 10^{-3} \cdot 25 \cdot 10^{-3} = 1.822 \cdot 10^{-3} \tag{97}$$

Compared to the figure and to Eq.(94) it is seen, that the results are consistent with the assumptions. To complete the bias design we assume that the base-emitter voltage under small signal conditions is V_{b00}=0.65 V. As discussed in section 5-3 on page 5.53, the voltage is reduced by an amount ΔV_{b0} given through

$$z \equiv \frac{\Delta V_{b0}}{V_t} \qquad where \qquad e^z = \frac{G_m}{g_m}\frac{x}{2\hat{I}_1(x)} = \frac{1}{3}\frac{6}{2 \cdot 61} = \frac{1}{61} \quad \Rightarrow$$
$$\Delta V_{b0} = -Vt \log 61 = -0.025 \cdot 4.11 = -0.102\,[V] \tag{98}$$

Thus, the base should be biased to

$$V_{bb} = V_{E0} + V_{b00} + \Delta V_{b0} = 1.3 + 0.65 - 0.1 = 1.85\,[V]\,. \tag{99}$$

The DC base-current under oscillations is I_{c0}/β=1.997/60=0.033 mA. We let the current through the bias resistors be more than ten times as large, namely I_{br}= 0.5mA. Then the current through R_{b2} is approximately the same as the current through R_{b1}, and we get

$$R_\Sigma \equiv R_{b1} + R_{b2} = \frac{V_{CC}}{I_{br}} = \frac{3.5}{0.5\cdot 10^{-3}} = 7.0\cdot 10^3 \Rightarrow$$

$$R_{b2} = \frac{V_{bb}}{V_{cc}} R_\Sigma = \frac{1.85}{3.5} 7.0\cdot 10^3 = 3.7\,[k\Omega], \qquad R_{b1} = R_\Sigma - R_{b2} = 7.0 - 3.7 = 3.3\,[k\Omega] \tag{100}$$

The parallel connection of R_{b1}, R_{b2}, and the large signal input resistance $R_{\pi 1}$ from Eq.(96) contributes to Q-factor. Since they are placed across capacitor C_b, we get

$$R_{bb} = R_{b1} \| R_{b2} \| R_{\pi 1} = \frac{1}{1/R_{b1} + 1/R_{b2} + 1/R_{\pi 1}} = \frac{1}{1/3.7 + 1/3.3 + 1/2.469} = 1.022\,[k\Omega]$$

$$R_{ser,bb} = \frac{1}{\omega_0^2 C_b^2 R_{bb}} = 0.5\cdot 10^{-3}, \tag{101}$$

$$Q_{int,bb} = \frac{1}{\omega_0^2 C_{ser}^2 R_{ser}} = \frac{1}{(2\pi 10^7)^2 .5\cdot 10^{-3}} = 3.267\cdot 10^4 .$$

This is a high Q-factor compared to the assumed value of $Q_{int} = 120$, so the transistor input and biasing resistors contribute nothing to the losses compared with the inductor loss. The parallel loss R_{int} comes from tuning inductor L_C has Q_L=150, and a corresponding parallel resistance,

$$R_{pL} = Q_L\ \omega_0 L_C = 150\cdot 2\pi\ 10^7 \cdot 260.0\,10^{-9} = 2.450\cdot 10^3 \sim 2.45\,[k\Omega], \tag{102}$$

so within the design above, there is room for a loss introduced by the RF choke L_{rcf}. Its parallel resistance may go down to

$$R_{p,rfc} = \frac{R_{int} R_{pL}}{R_{pL} - R_{int}} = \frac{1.531\cdot 2.450}{2.450 - 1.531} = 4.081\,[k\Omega] . \tag{103}$$

To complete the design, coupling capacitor C_{cp2} should not contribute to the tuning so it must be large compared C_{ser} from Eq.(92), say C_{cp2}=100nF. The reactance of coupling capacitor C_{cp3} should be small compared to the load resistor R_A, i.e.

$$\frac{1}{C_{cp3}\omega_0} \ll R_A \quad \Rightarrow \quad C_{cp3} \gg \frac{1}{\omega_0 R_A} = \frac{1}{2\pi 10^7 \cdot 600} = 26.5\,[pF] : \quad C_{cp3} = 2.7[nF]. \tag{104}$$

Finally C_{cp1} must bypass R_E. Since the time constant of $\tau_E = R_E C_{cp1}$ directly influence the gain regulation in G_m, the capacitance should not be chosen too high in order to avoid the squegging type of amplitude instability. According to the discussion in Appendix VI-A, a safe choise is to set the time constant τ_E equal to the logarithmic decrement of the resonance circuit. Thereby we get

$$\tau_E = \boldsymbol{R}_E C_{cp1} = \tau_Q = \frac{2Q}{\omega_0}\ , \qquad \Rightarrow \tag{105}$$

$$C_{cp1} = \frac{2Q}{\omega_0 \boldsymbol{R}_E} = \frac{2 \cdot 32.18}{2\,\pi\, 10^7 \cdot 640} = 1.60 \cdot 10^{-9} \sim 1.60[nF]\ .$$

Capacitor C_{cp1} controls the time constant in the gain control of the transistor under large signal operations in a manner that can be foreseen. However, the two coupling capacitors C_{cp2} and C_{cp3} might also contributes to this control, but it is difficult to work out the details analytically. The values that were calculated formerly did not incorporate any stability concerns, so we must be prepared to adjust the capacitor values when the circuit is build in practice or simulated to check performance. The latter is done in Fig.26, and there are no indications of amplitude instabilities in this design.

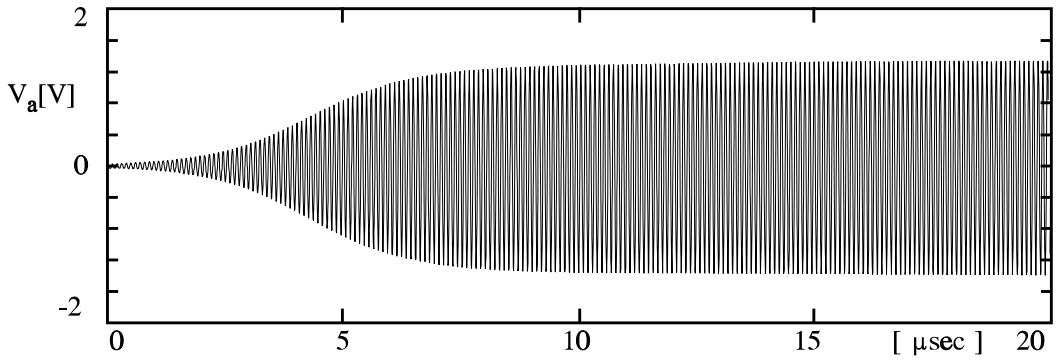

Fig.26 Build-up of oscillations in the Pierce oscillator from Fig.25 using the component values that were calculated in the example.

Example VI-2-2 end

VI-3 Crystal Oscillators

Quartz is a piezo-electrical material where mechanical deformations cause voltage differences across distinct surfaces and visa versa. A small sheet of quartz exhibits mechanical resonant modes that depend on its geometry, the orientation of the cut compared to the crystal axes, and the type of vibration engaged like compression, torsion, or shear oscillations. With two electrodes evaporated on the crystal, we get a component that typically has an impedance pattern as sketched in Fig.27. It shows pronounced resonances at the fundamental frequency and odd numbered overtones. Even numbered mechanical modes make no resultant displacement of the electrodes and cannot be exited electrically. Between dominant modes spurious resonances from other type of vibrations may be observed. Mechanical resonances have generally high Q-values and combined with excellent temperature stability and long-term aging properties, the quartz crystal is widely used as the frequency controlling element in oscillators that operates within close tolerances in the frequency range of .1 to approximately 350 MHz.

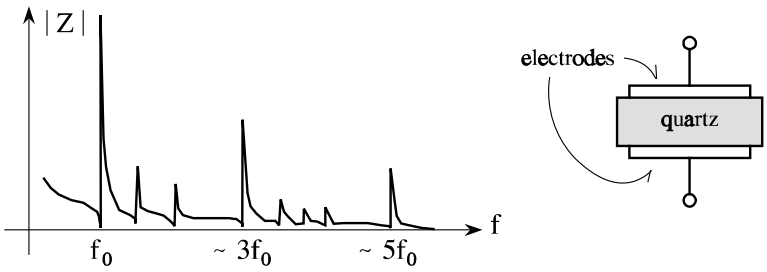

Fig.27 Impedance magnitude of quartz crystal with strong resonances at the fundamental mode and odd overtones. In between spurious resonances from other types of vibrations may be observed.

Crystal Equivalent Circuits

From an electrical point of view, the quartz crystal may be represented by the equivalent circuit in Fig.28(a), where the capacitor C_0 is the capacitance between the electrodes if there were no mechanical resonances. Each series resonant circuit C_i, L_i, r_i, represent a mechanical mode that may be excited by the piezo-electric effect. Commonly crystals are

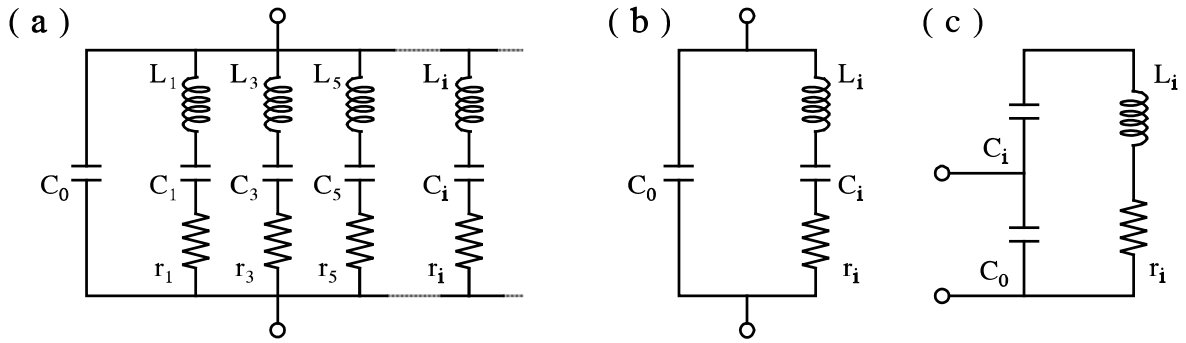

Fig.28 Electrical equivalent circuit of a quarts crystal. (a) includes all modes and (b) suffices for narrowband calculations with a particular mode. (c) is a redrawing of (b) emphasizing its parallel resonance.

optimized with respect to a particular mode that is recommended for circuit design. In the frequency range around the selected mode, it suffices to consider an equivalent circuit composed of only the electrode capacitance and the series circuit associated with the mode in question. This circuit is shown in Fig.28(b) and has the impedance,

$$Z_c(s) = \frac{1}{sC_0 + \dfrac{1}{1/sC_i + sL_i + r_i}} = \frac{s^2 + s\, r_i/L_i + 1/L_iC_i}{sC_0\left\{ s^2 + s\, r_i/L_i + (C_0+C_i)/L_iC_iC_0 \right\}} \tag{106}$$

$$= \frac{s^2 + s\,\omega_0/Q + \omega_0^2}{s\,C_0\left\{ s^2 + s\,\omega_0/Q + \omega_0^2\left[1 + C_i/C_0 \right] \right\}}$$

The last expression introduces the series resonance frequency ω_0 and the corresponding Q-factor of the series circuit,

$$\omega_0 \equiv 1/\sqrt{L_i C_i}\ , \qquad Q \equiv L_i\omega_0 / r_i = 1/C_i\omega_0 r_i\,. \tag{107}$$

Setting the numerator and the denominator in Eq.(106) equal to zero and solving for s, we get the impedance zeros and poles,

$$\textit{zeros}: \quad s_{z1,2} = -\frac{\omega_0}{2Q} \pm j\omega_0\sqrt{1-\frac{1}{4Q^2}} \approx -\frac{\omega_0}{2Q} \pm j\omega_0 \tag{108}$$

$$\textit{poles}: \begin{cases} s_{p0} = 0. \\ s_{p1,2} = -\dfrac{\omega_0}{2Q} \pm j\omega_0\sqrt{1+\dfrac{C_i}{C_0}-\dfrac{1}{4Q^2}} \approx -\dfrac{\omega_0}{2Q} \pm j\omega_0\left(1+\dfrac{C_i}{2C_0}\right) \end{cases}$$

Practical data justify the approximations, which imply large Q-factors. Extremely high Q´s are obtainable with crystals - up to 100000 - so the small losses get no influence on the imaginary parts of poles and zeros. Moreover, the electrode capacitance is much greater than any resonator capacitance and we may use the estimation

$$\sqrt{1+x} \approx 1 + x/2 \qquad \textit{for} \quad |x| \ll 1 \tag{109}$$

in the last expression, which determines a parallel resonance frequency - sometimes also called the antiresonance frequency - ω_p, where

$$\textit{parallel resonance}: \quad \omega_p \approx \omega_0\left(1+\frac{C_i}{2C_0}\right)\Bigg|_{C_0 \gg C_i} \tag{110}$$

The series resonance is responsible for the zero of the impedance function. In conjunction with the electrode capacitance C_0 it also provides the pole that implies the parallel resonance, which may be viewed upon like a parallel resonant circuit with capacitive transformation as shown in Fig.28(c).

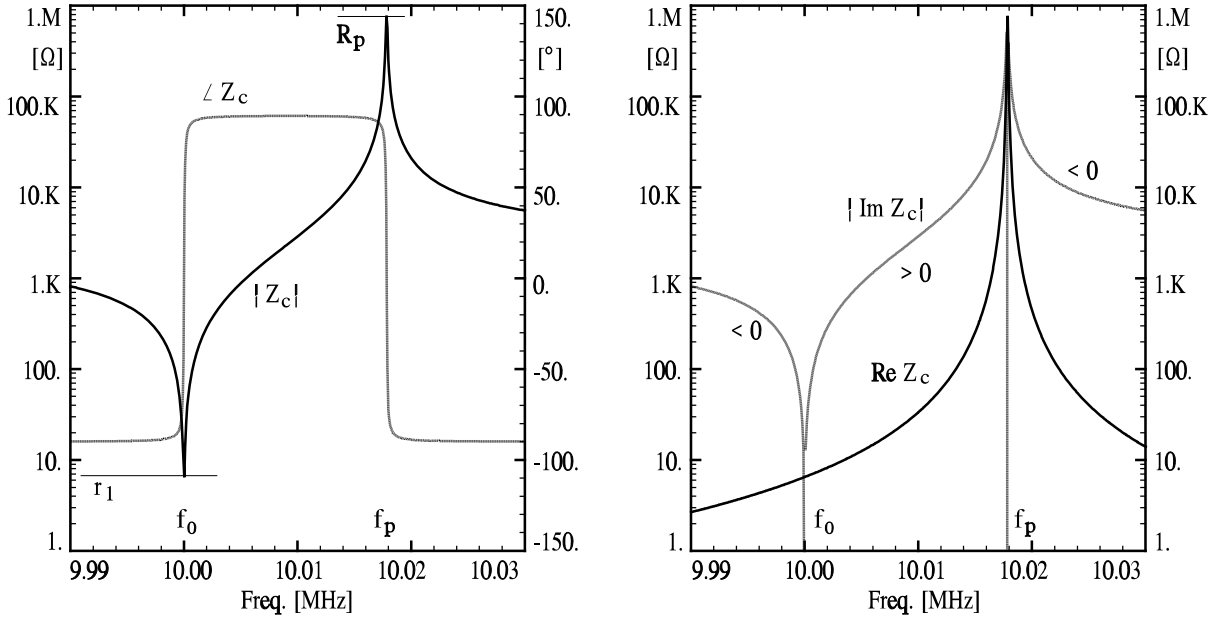

Fig.29 Impedance in magnitude, phase and in real, imaginary forms for the crystal example in Eq.(111). Note the logarithmic impedance scales and the sign indications for the imaginary part of the impedance.

Crystal data example, TeleQuartz TQ 10 05 18 10.000kHz (fundamental mode)

$$f_0 = 10.0\ MHz, \quad C_0 = 7.0\ pF, \quad r_1 = 6.5\ \Omega, \quad C_1 = 25.0\ fF, \quad \Rightarrow \quad L_1 = 10.13\ mH$$

$$Q = \frac{2\pi f_0 L_1}{r_1} = 97940\ , \qquad \frac{f_0}{2Q} = 51.05\ Hz\ , \qquad f_p - f_0 = f_0 \frac{C_1}{2C_0} = 17.9\ kHz \tag{111}$$

$$M = \frac{2Q(f_p - f_0)}{f_0} = 350.6\ , \qquad \textit{Drive Power}: \ P_q = 0.1\ mW$$

$$\textit{Tolerance}: \frac{\Delta f_0}{f_0} = 5.\ 10^{-6}, \qquad \textit{Temp.drift}: \frac{\Delta f_0}{f_0} = 5.\ 10^{-6},\ -20°C < T < 70°C$$

Due to the existence of both series and parallel resonances there may be two ways of utilizing a crystal in an oscillator, either as a low impedance devices in series resonance around ω_0 or as a high, inductive impedance device in parallel resonance up to ω_p. The possibilities are readily seen in Fig.29, which shows a calculation of the impedance function from Eq.(106) based on the crystal data in Eq.(111). With practical data, the series and parallel resonances are closely spaced in frequency. In this case, however, the distance is still large compared to the real part of poles and zeros, so the two resonances are clearly distinguishable. The separation may be expressed through the following figure of merit M,

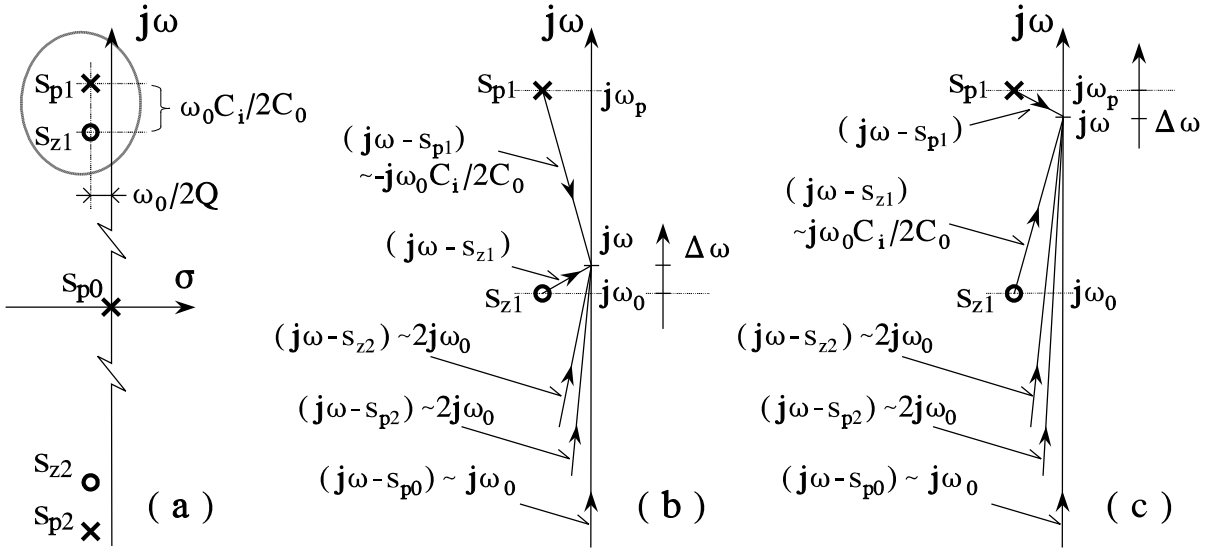

Fig.30 Pole-zero pattern for a single resonant mode in the crystal. The encircled region is shown in (b) for series and (c) for parallel resonances and indicate phasor assumptions in narrowband approximations.

$$M \equiv \frac{2Q}{\omega_0}(\omega_p - \omega_0) = \frac{QC_i}{C_0} = \frac{1}{C_0\omega_0 r_i}, \tag{112}$$

where the distance ω_p-ω_0 is given through Eq.(110).

The two types of resonances in Fig.29 show both the steep phase characteristic that is required for good frequency stability. We chose between them in design by letting the rest of the circuit meet oscillation criteria with either high or low impedance levels. Crystals operated in fundamental mode have usually high M values. Therefore, the impedance may be narrowband approximated around either ω_0 or ω_p using the method that was applied to LC tuned circuits in section II-3. With known poles and zeros the crystal impedance is expressed

$$Z_c(\omega) = \frac{(j\omega - s_{z1})(j\omega - s_{z2})}{C_0(j\omega - s_{p0})(j\omega - s_{p1})(j\omega - s_{p2})}. \tag{113}$$

The pole-zero pattern for the crystal is shown in Fig.30(a) while Fig.30(b) and (c) indicate the geometry to be used in the narrowband approximation. Notice that the figures are not drawn to scale as the pole and zero distances to the imaginary axis should be much smaller compared to their mutual spacings. With the assumptions in the figures we get

$$Z_c(\omega) \approx \frac{(j\omega - s_{z1})\, 2j\omega_0}{C_0\, j\omega_0\, (j\omega - s_{p1})\, 2j\omega_0}$$

$$\begin{cases} \underset{series}{\approx} \dfrac{\omega_0/2Q + j(\omega-\omega_0)}{C_0\omega_0^2\, C_i/2C_0} = r_i \left\{ 1 + j\, Q\, \dfrac{2\Delta\omega}{\omega_0} \right\}, \quad \Delta\omega = \omega - \omega_0, & (a) \\ \underset{parallel}{\approx} \dfrac{j\omega_0\, C_i/2C_0}{C_0 j\omega_0\, (\omega_0/2Q + j(\omega-\omega_p))} = \dfrac{\dfrac{1}{r_i\,(C_0\omega_0)^2}}{\left\{ 1 + j\, Q\, \dfrac{2\Delta\omega}{\omega_0} \right\}}, \quad \Delta\omega = \omega - \omega_p. & (b) \end{cases}$$

(114)

It is seen that the two narrowband approximations in (a) and (b) are of the same form as the approximations that were derived for simple resonance circuits in section II-3[2]. The two resonance frequencies ω_0 and ω_p are so close that they are taken equal unless we are considering the deviation $\Delta\omega$ from the either the series or the parallel resonance frequency.

The series resonance in Eq.(114)a is independent of the electrode capacitance C_0. In parallel resonance the electrode capacitance determines the equivalent parallel resistance, which is the numerator in Eq.(114)b,

$$R_p = \frac{1}{(C_0\omega_0)^2\, r_i}, \qquad example:\ R_p = \frac{1}{\left[7\times10^{-12}\, 2\pi\, 10\times10^6\right]^2 6.5} = 795.3\ k\Omega\ , \quad (115)$$

where the numerical example corresponds to the crystal data in (111). This resistance value is recognized as the peak impedance in Fig.29. The final expressions in Eq.(114) may also be represented by narrowband equivalent circuits given by Fig.30. In series mode the crystal is represented by a small resistance in series with a resonant reactance, in parallel mode by a large resistor in parallel to a resonant susceptance.

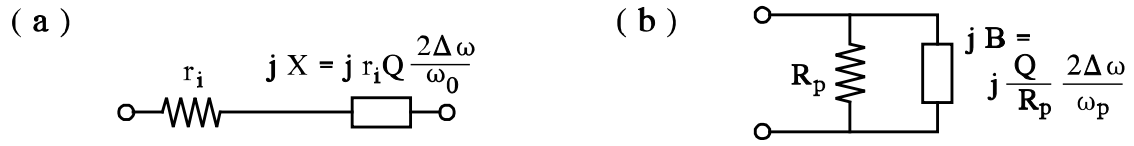

Fig.31 Narrowband equivalents of the crystal in series (a) and parallel (c) resonance modes.

---

2) The validity of the narrowband approximation for the equivalent circuit in Fig.28b is implicitly the reason why all parallel resonators in Fig.28a excepts the one selected may be disregarded. They contribute only canceling pole-zero pairs if they are incorporated in Eq.(113).

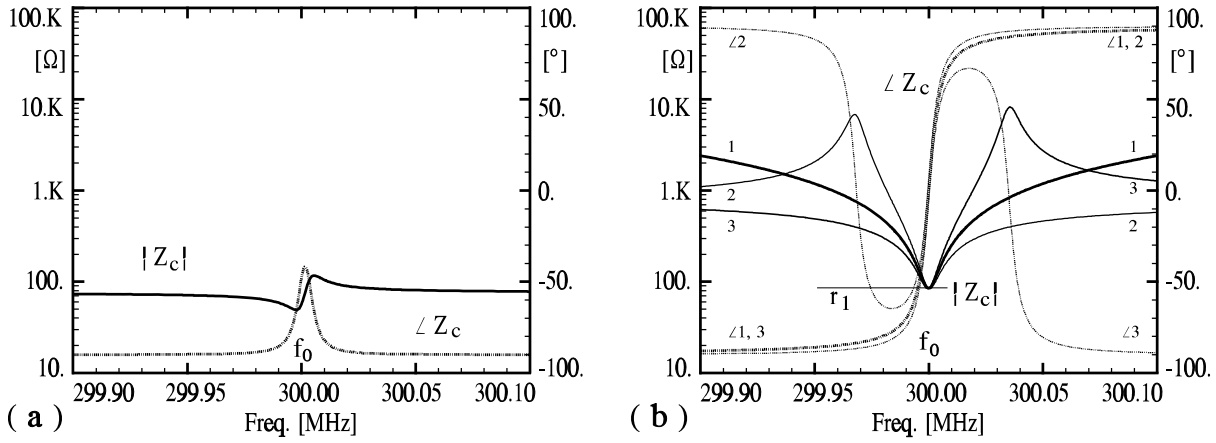

Fig.32 Impedance magnitude and phase of a low-M crystal before and after inductive compensation. Three cases are shown, 1) L_p set exactly to, 2) 10% over, and 3) 10% below the ideal value.

Crystal data example, TeleQuartz TQ 18 07 18 300.000*kHz* (*9´th overtone*)

$$f_0 = 300.0\ MHz, \quad C_0 = 7.0\ pF, \quad r_1 = 85\ \Omega, \quad C_1 = 0.15\ fF, \quad \Rightarrow \quad L_1 = 1.876\ mH$$

$$Q = \frac{2\pi f_0 L_1}{r_1} = 41610\ , \qquad \frac{f_0}{2Q} = 3.605\ kHz\ , \qquad f_p - f_0 = f_0\,\frac{C_1}{2C_0} = 3.214\ kHz \tag{116}$$

$$M = \frac{2Q\,(f_p - f_0)}{f_0} = 0.8916\ , \qquad L_p = \frac{1}{(2\pi f_0)^2 C_0} = 40.21\ nH\ ,$$

Overtone crystals have commonly smaller relative distances between the series and parallel resonances - the higher the mode number, the smaller the distance. This is exemplified by ninth overtone crystal data in (115), where the figure of merit M from Eq.(112) even falls below one, so the zero and pole separation along the imaginary axis is smaller than the distance to the imaginary axis. With M approaching zero the contributions from all resonance pole-zero pairs to the crystal impedance through Eq.(113) tend to cancel each other, so all what will be left is the shunting impedance of the electrode capacitance. With exception of modest deviations closely around f_0, the shunting effect of C_0 dominates the patterns in Fig.32(a), which show simulations based on data in the example. According to Eq.(112), M may also be interpreted as the ratio of the electrode impedance over the series circuit impedance at ω_0. To get a distinct frequency response that may serve for oscillator design with a low M value crystal, the effect of the electrode capacitance must be compensated. One obvious way to do so is to neutralize C_0 by a parallel inductance L_p as shown in Fig.33. If the tuning is exact,

$$L_p = \frac{1}{C_0\,\omega_0^2}\ , \tag{117}$$

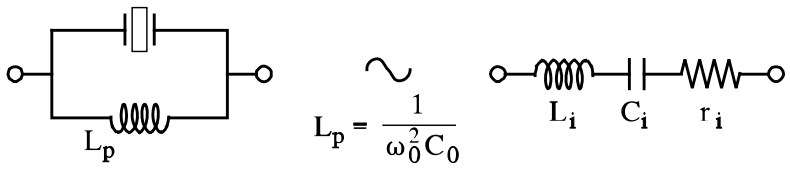

Fig.33 Compensation of electrode capacitance by a parallel inductance in a low-M crystal.

only the series resonant circuit remains and may be used as an equivalent circuit around ω_0. However, a less precise compensation still works if the impedance of C_0 paralleled by L_p is large compared to r_i. Then the series resonance pattern - distinct magnitude minimum and steep rise in phase - prevails as seen in the characteristics of Fig.32(b), where all examples coincide around f_0.

Loading and Driving Crystals

To benefit from crystals in oscillator design, it is important to keep the Q-factor high. Compared to the Q-factor of the crystal itself, which in the present context often is referred to as the unloaded Q, some reductions are unavoidable when the crystal is connected to the remaining part of the oscillator circuit, which contains transistor impedances, biasing networks, and the external load. If the losses transform to a series resistor r_L in a crystal that is used in series mode, Fig.34(a), the resultant Q-factor is the one we get by adding the external resistor to the internal resistor in Eq.(107), i.e.

$$Q_s = \frac{L_i \omega_0}{r_s} = \frac{r_i}{r_s} Q_{unloaded}, \qquad where \qquad r_s = r_i + r_L . \tag{118}$$

Correspondingly, if the external losses may be represented by a parallel resistance R_L to a crystal that is operated in parallel mode, the resultant Q-factor is the one we get from paralleling the external resistance to the parallel resistance R_p, Eq.(115),

$$Q_t = \frac{R_t}{R_p} Q_{unloaded}, \qquad where \qquad R_t = \frac{R_L R_p}{R_L + R_p} . \tag{119}$$

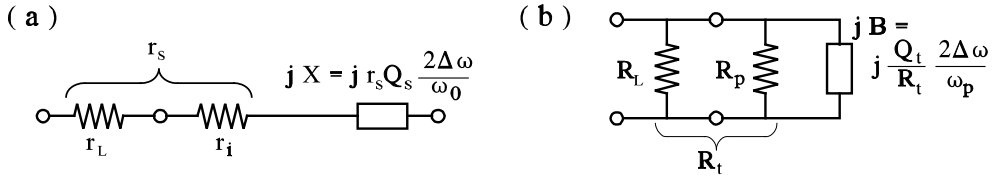

Fig.34 Resistive reduction of the Q-factors in series (a) and parallel (b) resonance modes.

Reactive loading of the crystals may change both resonance frequencies and Q-factors. In some situations this is an unavoidable imperfection but adding a capacitance in

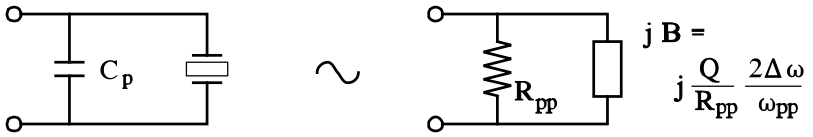

Fig.35 Equivalent representation of a capacitance in parallel with a crystal.

series or parallel to a crystal may also be a mean for external adjustments of the resonance frequencies. The simplest reactive loading situation is the one where a capacitor C_p is connected in parallel to the crystal because C_p simply adds to the electrode capacitance C_0. All we have to do is to replace C_0 in the initial developments from Eqs.(106) to (110) with C_0+C_p. Thus, the new parallel resonance frequency ω_{pp} becomes

$$\omega_{pp} \approx \omega_0 \left(1 + \frac{C_i}{2(C_0+C_p)} \right) \quad \Rightarrow \quad \begin{cases} C_p \to 0: & \omega_{pp} \to \omega_p \ , \\ C_p \to \infty: & \omega_{pp} \to \omega_0 \ . \end{cases} \tag{120}$$

As seen, ω_{pp} is lowered from its unloaded value in Eq.(110) towards the series resonance frequency ω_0, which is approached in the theoretical limit of $C_p \to \infty$. In this context, the frequency interval f_p - f_o is called the pulling range of the crystal. The range cannot be fully exploited as the figure of merit in Eq.(112), with the effect of C_p included, must stay well above 1 to keep the parallel resonance defined. Electrode capacitance C_0 had no influence on the real part of the poles and zeros. This will neither be the case when C_p is added, so the Q-factor remains unaffected of a parallel capacitor. However, the resultant parallel resistance is changed and given by Eq.(115) using C_0+C_p instead of C_0. The crystal and capacitance in parallel connection gets the equivalent representation in Fig.35, where

$$R_{pp} = \frac{1}{r_i (C_p + C_0)^2 \omega_{pp}^2} \ . \tag{121}$$

Another view upon the parallel connection of a crystal and a capacitor is illuminated by Fig.36. It takes outset in the common way of employing a parallel resonant crystals as replacements for the coil in oscillator circuits since the crystal is inductive between f_p and f_o. Starting from a LC oscillator designed to operate at frequency ω_{pp} with a tuning capacitance

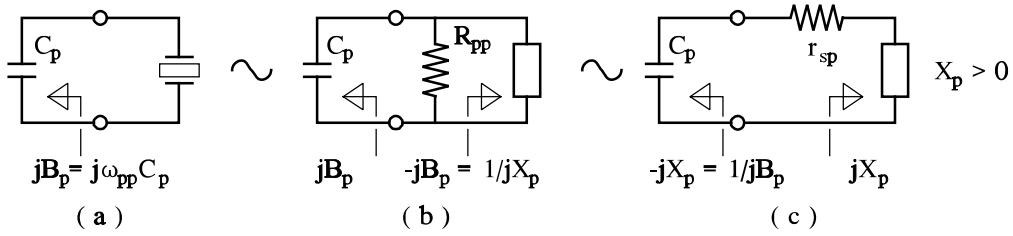

Fig.36 Series resistance evaluation for a crystal used in parallel mode as a coil replacement.

equal to C_p and susceptance B_p, the canceling negative susceptance $-B_p$ from the inductance may instead be provided by the crystal to get improved stability[3]. Although the crystal is utilized in its parallel mode, the resonance circuit in the oscillator may be of either series or parallel form. In the first case, losses are represented by parallel resistance R_{pp} from Eq.(121). With series circuits it may be more convenient to consider series components as indicated in Fig.36(c). Using the series-to-parallel conversions, the equivalent series resistance is given by

$$r_{sp} = \frac{X_p^2}{R_{pp}} = r_i \left[\frac{C_p + C_0}{C_p} \right]^2 . \tag{122}$$

If a capacitance C_s is placed in series with the crystal that is not inductively compensated, Fig.37(a), we get the impedance function

$$Z_s(s) = \frac{1}{sC_s} + Z_c(s) = \frac{1}{sC_s} + \frac{s^2 + s\omega_0/Q + \omega_0^2}{sC_0 \left\{ s^2 + s\omega_0/Q + \omega_0^2 \left[1 + C_i/C_0 \right] \right\}}$$

$$= \frac{s^3 (C_0 + C_s) + s^2 \omega_0 (C_0 + C_s)/Q + s\,\omega_0^2 (C_0 + C_s + C_i)}{s^2 C_s C_0 \left\{ s^2 + s\,\omega_0/Q + \omega_0^2 \left[1 + C_i/C_0 \right] \right\}} \tag{123}$$

$$= \frac{s^2 + s\,\omega_0/Q + \omega_0^2 \left[1 + C_i/(C_0 + C_s) \right]}{s\,C_0C_s/(C_0 + C_s) \left\{ s^2 + s\,\omega_0/Q + \omega_0^2 \left[1 + C_i/C_0 \right] \right\}} .$$

Compared with the impedance Z_c of the crystal itself from Eq.(106), it is seen that the denominator will leave the poles unaffected. The new zeros become

$$zeros\,|_{C_s}: s_{0s} = -\frac{\omega_0}{2Q} \pm j\omega_0 \sqrt{1 + \frac{C_i}{C_0 + C_s} - \frac{1}{4Q^2}} \approx -\frac{\omega_0}{2Q} \pm j\omega_0 \left(1 + \frac{C_i}{2(C_0 + C_s)} \right) \tag{124}$$

There are no changes in the real part of the zeros due to the series capacitance C_s so Q is unchanged. The imaginary part, which determines the series resonance frequency, is enlarged, but it is seen that the pulling range is again the interval between frequencies f_p and f_o,

$$\omega_{0s} = \omega_0 \sqrt{1 + \frac{C_i}{C_0 + C_s}} \approx \omega_0 \left(1 + \frac{C_i}{2(C_0 + C_s)} \right) \quad \Rightarrow \quad \begin{cases} C_s \to 0: & \omega_{0s} \to \omega_p , \\ C_s \to \infty: & \omega_{0s} \to \omega_0 . \end{cases} \tag{125}$$

---

3) Crystals may be optimized and specified for parallel usage, given the resonance frequency f_{pp} and the required parallel capacitance. The latter is commonly called the load capacitance of the crystal in data sheets.

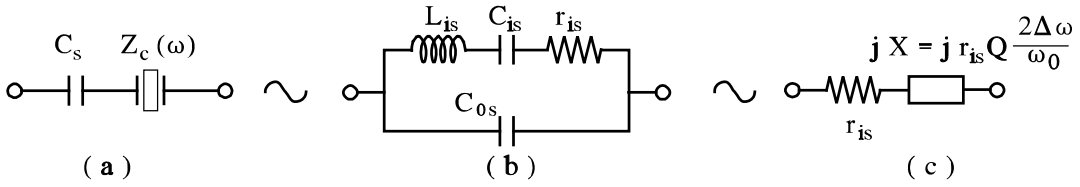

Fig.37 Equivalent circuits for a capacitor and a crystal in series connection. The component values are defined in Eqs.(126) and (128).

With a series capacitor it is possible to control the series resonance frequency where the crystal has minimum impedance. Exactly how low it is may be crucial for setting up the gain requirement in an oscillator. To find the series resistance we use the following rewriting,

$$\omega_{0s}^2 = \omega_0^2 \left(1 + \frac{C_i}{C_0 + C_s} \right), \qquad n = \frac{C_0 + C_s}{C_s}, \qquad r_{is} = r_i \, n^2,$$

$$L_{is} = L_i \, n^2, \qquad C_{0s} = \frac{C_0}{n} = \frac{C_0 C_s}{C_0 + C_s}, \qquad C_{is} = \frac{C_i}{n^2} \frac{\omega_0^2}{\omega_{0s}^2}, \qquad (126)$$

$$Q_s = \frac{L_{is}\omega_{0s}}{r_{is}} = Q \frac{\omega_0}{\omega_{0s}} \approx Q .$$

Direct substitution of these relations into the last part of Eq.(123) yields

$$Z_s(s) = \frac{s^2 + s\,\omega_{0s}/Q_s + \omega_{0s}^2}{s\,C_{0s}\left\{ s^2 + s\,\omega_{0s}/Q_s + \omega_{0s}^2 \left[1 + C_{is}/C_{0s} \right] \right\}}, \qquad (127)$$

This expression has exactly the same structure as the crystal impedance Z_c in Eq.(106), so the series connection may be represented equivalent circuits having the same topology as the crystal without the series capacitor, Fig.37(b) and (c), but clearly with different component values. In particular the new series resistor at resonance becomes

$$r_{is} = r_i \left(\frac{C_0 + C_s}{C_s} \right)^2 . \qquad (128)$$

Crystal Oscillator Circuits

Like the situation with LC oscillators, the number of circuits that are proposed for crystal oscillators is overwhelming, so again we can only consider a few types and examples. For a more complete presentation, which also includes temperature compensation techniques to meet tight tolerances, you should consult the specialized literature, for instant ref. [8].

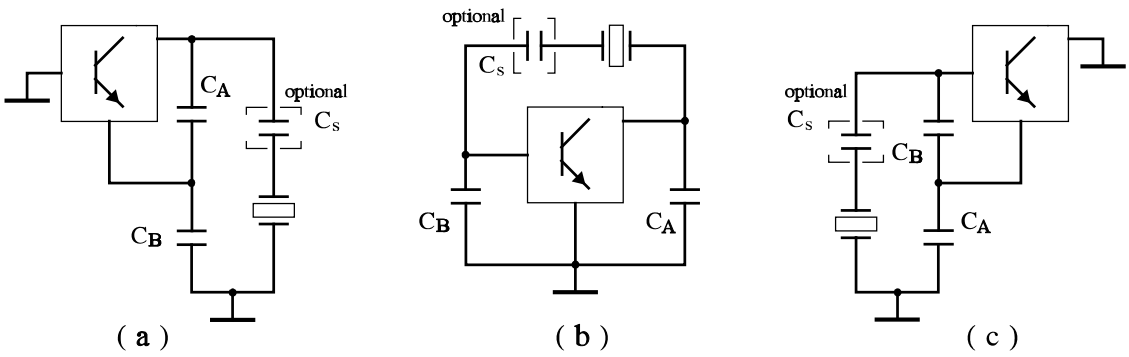

Fig.38 Colpitts (a), Pierce (b), and Seiler (c) oscillators where crystals have replaced the inductors of the LC circuits. The optional series capacitor may be inserted to tune frequency and/or transform impedance levels.

To get an idea on how crystals are used in oscillators, the examples in Fig.38 show the basic configuration that was introduced for LC oscillators in Fig.17, but now inductors are replaced by crystals. Here the crystals are used as high impedance, inductive devices that must tune to the capacitances at a frequency between the parallel and the series resonance of the crystal. To adjust frequency or impedance level or both, we may insert a capacitor C_S in series with the crystal as indicated in the figures. In these cases the crystal equivalent from Fig.37 and the related expressions may be used for the design.

Closely around series resonance, the crystal has a low impedance and may, therefore, be used to make a highly frequency selective closing of the feed-back loop in the oscillator. This is demonstrated in the examples of Fig.39, where the function of the crystal is to establish connection to the transistor output in some of the LC oscillator circuits we considered above. At a first glance we may suppose the LC resonance circuit is superfluous in these examples. However, we saw initially that a crystal has a fundamental mode and several odd-numbered overtones, each presenting an impedance minimum. The LC circuit, which should resonate around the desired oscillator frequency, gets the role of selecting the correct mode of the crystal.

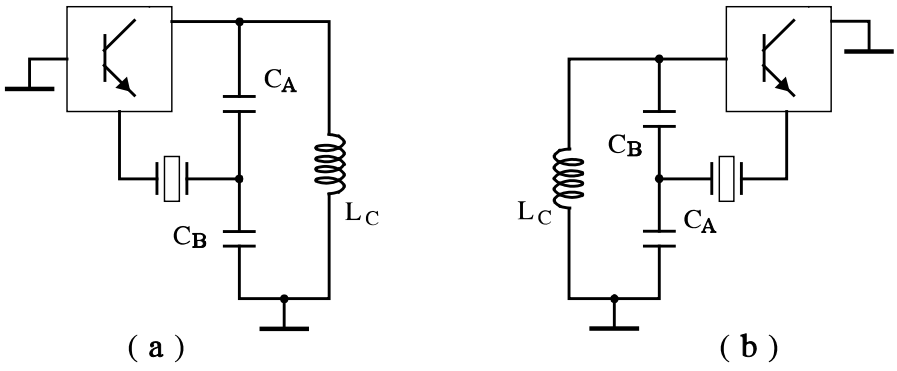

Fig.39 Colpitts (a) and Seiler (b) oscillators using crystals in low-impedance series modes to close the feed-back loop directly.

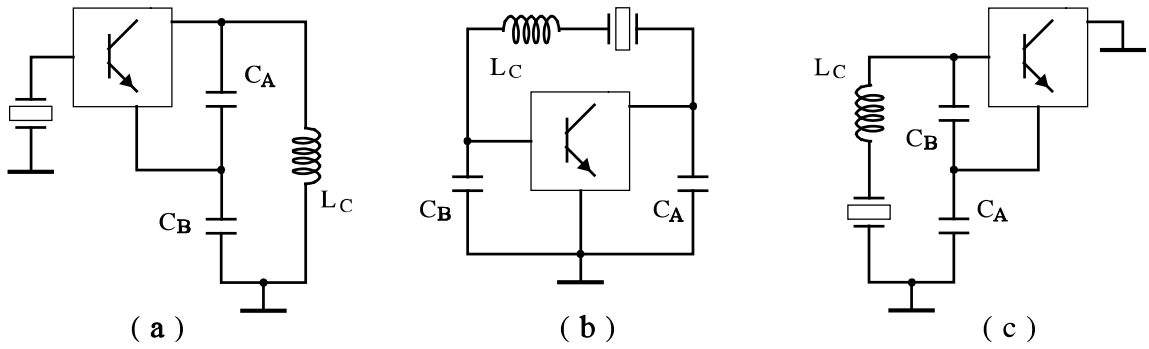

Fig.40 Colpitts (a), Pierce (b), and Seiler (c) oscillators where crystals are used in low impedance series mode to make highly frequency selective component connections.

Other ways of using a crystal in low impedance mode around the series resistance are demonstrated by Fig.40. The function of the circuit example in Fig.40(a) is that the crystal makes a frequency selective grounding of the base/gate terminal. In a narrow frequency band this establish the necessary gain in a Colpitts oscillator, where it is supposed that the active element operates in grounded base or gate configuration. In the two other examples, the crystal connects the inductor and compensates its inductance to provide oscillations close to the series resonance of the crystal. This technique is often referred to as impedance inversion since we use the crystal as a low impedance device in conjunction with an external inductor to establish a high inductive impedance. The method is often used in conjunction with overtone crystals since - according to the discussion in the example of Fig.32 - high impedance parallel modes may give difficulties in practical use.

Example VI-3-1 (IC-connected crystal oscillators)

A demonstration of crystal oscillator structures is given in Fig.41. It shows a block diagram of an IC circuit, which contains all active circuits that are required in a narrowband FM receiver. The circuit is intended for double conversion so it uses two intermediate frequencies and two local oscillators are required. They are denoted 1st LO and 2nd LO respectively where the first one uses impedance inversion of the type in Fig.40(c) and last one is of the type in Fig.38(c) without the series capacitance.

MOTOROLA

The MC13135/MC13136 are the second generation of single chip, dual conversion FM communications receivers developed by Motorola. Major improvements in signal handling, RSSI and first oscillator operation have been made. In addition, recovered audio distortion and audio drive have improved. Using Motorola's MOSAICE 1.5 process, these receivers offer low noise, high gain and stability over a wide operating voltage range.

Both the MC13135 and MC13136 include a Colpitts oscillator, VCO tuning diode, low noise first and second mixer and LO, high gain limiting IF, and RSSI. The MC13135 is designed for use with an LC quadrature detector and has an uncommitted op amp that can be used either for an RSSI buffer or as a data comparator. The MC13136 can be used with either a ceramic discriminator or an LC quad coil and the op amp is internally connected for a voltage buffered RSSI output.

These devices can be used as stand±alone VHF receivers or as the lower IF of a triple conversion system. Applications include cordless telephones, short range data links, walkie±talkies, low cost land mobile, amateur radio receivers, baby monitors and scanners.

- Complete Dual Conversion FM Receiver ± Antenna to Audio Output
- Input Frequency Range ± 200 MHz
- Voltage Buffered RSSI with 70 dB of Usable Range
- Low Voltage Operation ± 2.0 to 6.0 Vdc (2 Cell NiCad Supply)
- Low Current Drain ± 3.5 mA Typ
- Low Impedance Audio Output < 25 Ω
- VHF Colpitts First LO for Crystal or VCO Operation
- Isolated Tuning Diode
- Buffered First LO Output to Drive CMOS PLL Synthesizer

MC13135 MC13136

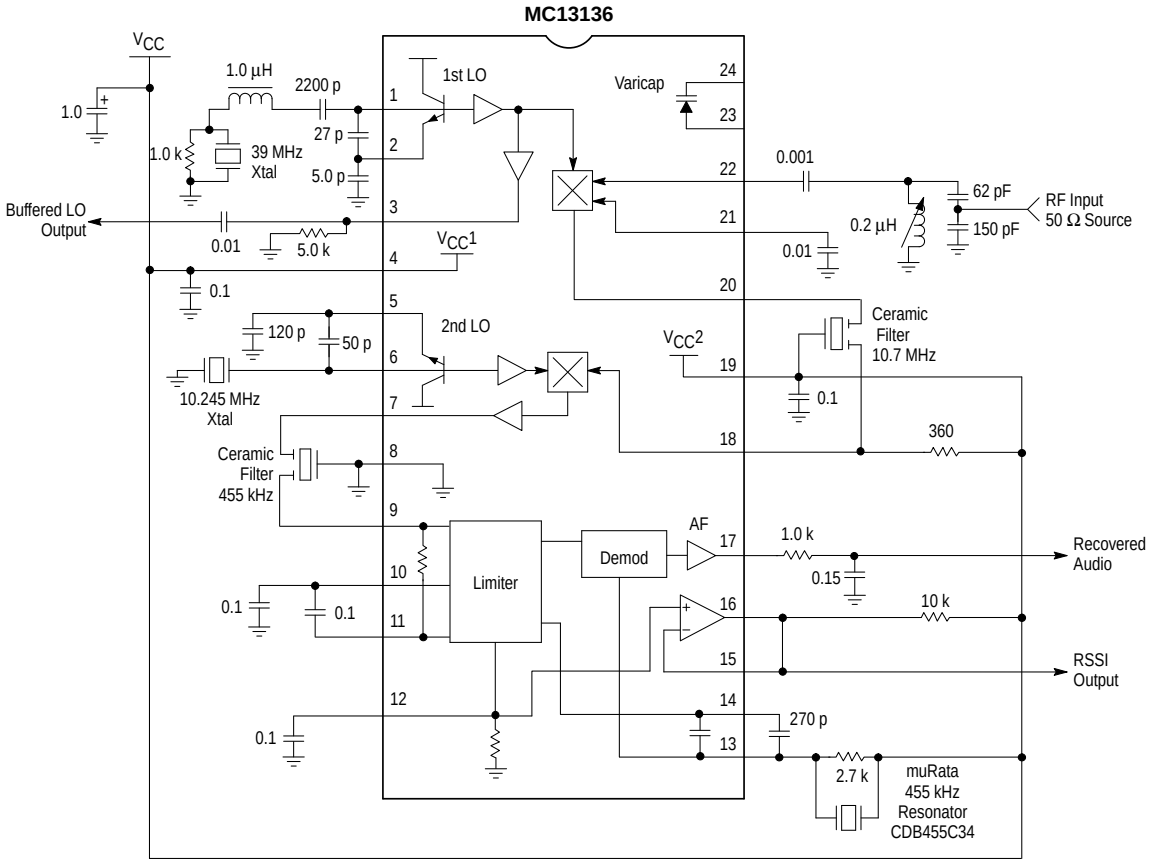

Figure 20a. Single Channel Narrowband FM Receiver at 49.7 MHz

Fig.41 Extracts from Motorola's online IC selection guide. Capacitances are in µF unless it is specified otherwise

Example VI-3-1 end

APPENDIX VI-A Oscillator Amplitude Stability

To present and investigate the amplitude stability problem in the sinusoidal prototype oscillator from Fig.3 we consider the block-diagram in Fig.42(a). Here, the transistor is characterized by the relationships between DC and fundamental frequency input voltages and the corresponding collector or emitter current components. The relations were formerly expressed by Eqs.(5-40) to (5-46). In summary the expressions that are needed below read,

$$I_{e0} = I_{ES}\, e^{V_{b0}/V_t}\, \hat{I}_0(x), \qquad I_{c1} = \alpha_f I_{ES}\, e^{V_{b0}/V_t}\, 2\,\hat{I}_1(x), \qquad where \quad x = V_{b1}/V_t\ . \tag{129}$$

The hatted quantities $\hat{I}_1$ and $\hat{I}_0$ are the modified Bessel functions of order one and zero respectively and α_f=1-1/β_f is the common base current gain, which is close to but slightly below one. The block representing the tuned circuit in the diagram relates fundamental frequency amplitudes. According to sect.II-1, the voltage amplitude in response to a current amplitude at resonance is expressed in Laplacian terms by a single time constant

$$V_{out}(s) = \frac{R_p}{1 + s\,\tau_Q}\, I_{c1}(s)\ , \qquad where \qquad \tau_Q = \frac{2Q}{\omega_0} = 2\,R_p C\ . \tag{130}$$

The DC biasing relationship is expressed through the impedance in series with the emitter, which is also a single time constant relationship

$$V_E(s) = \frac{R_E}{1 + s\,\tau_E}\, I_{c0}(s)\ , \qquad where \qquad \tau_E = R_E C_E\ . \tag{131}$$

While τ_Q represents the maximum rate of amplitude variations across the resonance circuit, τ_E sets the rate by which the oscillator circuit attempt to control this amplitude. To succeed, the two time constant must be comparable in size. If the amplitude control is too slow the amplitude will vary periodically in time as illustrated in Fig.9(b). If, on the other hand, τ_E is

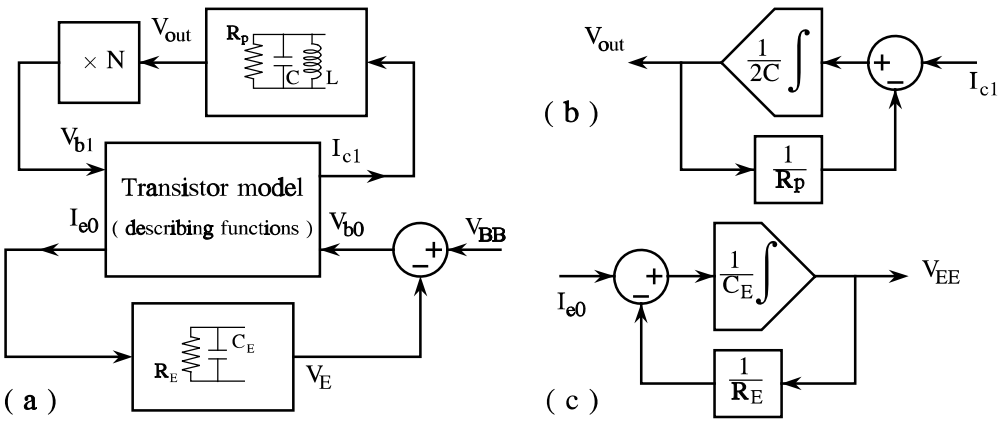

Fig.42 Block-diagram representation of oscillator amplitude control. To conduct a dynamic simulation, the two generic blocks in (a) must be replaced by the integration blocks in (b) and (c).

too short the emitter decoupling becomes insufficient and the circuit may either start oscillating with low amplitude at a wrong frequency or not start at all. As will be discussed below, a good design choice is to set the two time constants equal, like it was done to get the smooth amplitude start-up in Fig.9(a).

The time constant expressions in Eqs.(130),(131) are s-domain versions of the time-domain relationships that are shown in Fig.42(b) and (c), which are necessary to conduct calculations on how the oscillator amplitude evolves in time. With two integrators, the problem to be solved is a second order differential equation. It is nonlinear due to the nonlinear relationships in the transistor description from Eq.(129) and no simple solution exists. We shall, however, assume that such a solution with amplitude V_{b1} has build up to formal stationarity where Barkhausen's criterion applies,

$$G_m(x)\,\boldsymbol{R}_p N = 1\,, \qquad x = V_{b1}/V_t\,. \tag{132}$$

If this solution is stable it is supposed that the oscillator amplitude remain stable when it is disturbed by small perturbations δV_{b1}. The question of amplitude stability is discussed from that point of view.

Linearizing around a given solution to find the current variation, which corresponds to an amplitude perturbation $\Delta I_{c1} = G_{\Delta 11}\delta V_{b1}$, may be represented by the block-scheme in Fig.43. Here, linearized transconductances G_{11} through G_{00} depend on the actual large signal voltages V_{b1} and V_{b0}, and the block-scheme or the flow-graph provide directly

$$G_{\Delta 11} \equiv \frac{\Delta I_{c1}}{\delta V_{b1}} = \frac{M}{D}\,, \qquad \textit{where} \qquad M = G_{11}\left(1 + \frac{G_{00}\boldsymbol{R}_E}{1+s\tau_E}\right) - \frac{G_{10}G_{01}\boldsymbol{R}_E}{1+s\tau_E}\,, \tag{133}$$

$$\boldsymbol{D} = 1 - \frac{G_{11}\boldsymbol{R}_p N}{1+s\tau_Q} + \frac{G_{00}\boldsymbol{R}_E}{1+s\tau_E} + \frac{G_{10}G_{01}\boldsymbol{R}_E\boldsymbol{R}_p N}{(1+s\tau_E)(1+s\tau_Q)} - \frac{G_{00}G_{11}\boldsymbol{R}_E\boldsymbol{R}_p N}{(1+s\tau_E)(1+s\tau_Q)}\,.$$

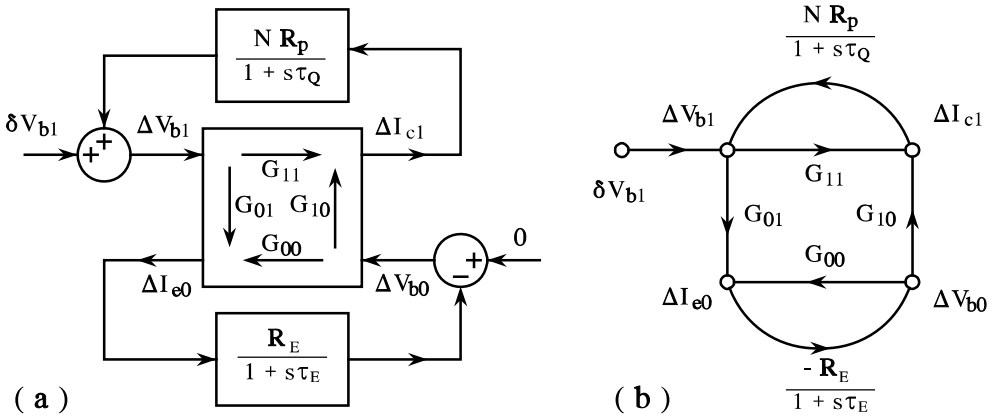

Fig.43 Linearization of the block-scheme from Fig.42 and the corresponding signal flow-graph. Both describe how small amplitude variations develop in oscillations .

Introducing the determinant

$$\Delta G = G_{11} G_{00} - G_{10} G_{01} \tag{134}$$

a reorganization including collection of terms in equal powers in s gives

$$G_{\Delta 11}(s) = G_{11} \frac{c + bs + as^2}{C + Bs + As^2}$$

$$= \frac{G_{11}\left(1 + \Delta G R_E / G_{11} + s\left[\tau_E + \tau_Q(1 + \Delta G R_E / G_{11})\right] + s^2 \tau_E \tau_Q\right)}{\left(\begin{array}{l} 1 - G_{11} R_p N + G_{00} R_E - \Delta G R_E R_p N \\ \qquad + s\left[\tau_Q(1 + G_{00} R_E) + \tau_E(1 - G_{11} R_p N)\right] + s^2 \tau_E \tau_Q \end{array}\right)} . \tag{135}$$

It is supposed that the response to an enforced amplitude pulse δV_{b1} should be stable and approach zero if the underlying large-signal oscillation is stable. The last condition is fulfilled if the transfer function is stable, since in that case we have,

$$\lim_{t \to \infty} \Delta I_{c1} = \lim_{s \to 0} s\, G_{\Delta 11}(s) = 0 . \tag{136}$$

Stability requires that the poles of the transfer function are in the left half-plane only, a condition that is met if all three coefficients in the second order denominator polynomial have equal and - following the second order term - positive signs.

To illuminate the role of the constant term C in the denominator of Eq.(135), which must be positive, we consider small stationary perturbations of the driving signal in the oscillator amplifier if no feedback for oscillation was established. The corresponding block-scheme and signal flow-graph are given in Fig.44, from which we derive the transfer function,

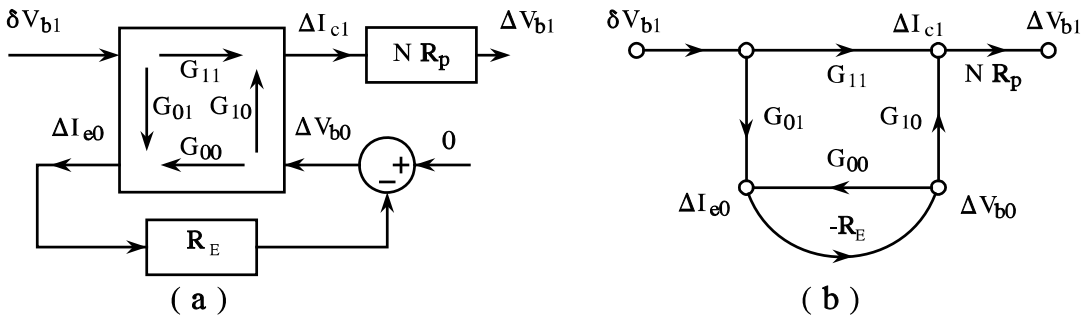

Fig.44 Linearized block-scheme and corresponding signal flow-graph for the oscillator amplifier without the upper oscillation feedback loop that is present in Fig.43.

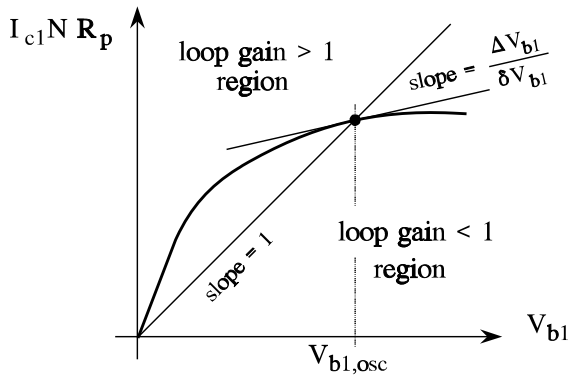

Fig.45 Stationary, large signal loop-gain response. Barkhausen's criterion is met at the unit slope line.

$$\left.\frac{\Delta V_{1b}}{\delta V_{1b}}\right|_{no\ osc.feeback} = R_p N\ \frac{G_{11}\left(1 + G_{00}R_E\right) - G_{01}G_{10}R_E}{1 + G_{00}R_E} = \frac{G_{11}R_pN + \Delta G R_E R_p N}{1 + G_{00}R_E}\ . \quad (137)$$

This ratio must be less than one in a self-limiting amplifier. It is the crossing slope of the stationary loop response curve at the stabilized amplitude, $V_{b1,osc}$, where the curve moves from the greater than one loop gain region to the smaller then one region as sketched in Fig.45. The condition is expressed

$$\left.\frac{\Delta V_{1b}}{\delta V_{1b}}\right|_{no\ osc.feeback} < 1 \quad \Rightarrow \quad C = 1 - G_{11}R_pN + G_{00}R_E - \Delta G R_E R_p N > 0. \quad (138)$$

The left hand side of this inequality is recognized as the constant denominator term. We have seen that it is positive if the amplifier is adequate for oscillator applications.

Investigating the first order coefficient B in the s term of the denominator from Eq.(135), it is useful to introduce the time constant ratio

$$K_\tau \equiv \tau_E / \tau_Q\ . \quad (139)$$

The condition to be fulfilled is written

$$B = \tau_Q\left[\ 1 + G_{00}R_E + K_\tau\left(\ 1 - G_{11}R_pN\ \right)\right] > 0 \ ? \quad (140)$$

a requirement that sets an upper bound on the time constant ratio

$$\underline{\textit{Amplitude Stability:}} \qquad K_\tau \equiv \frac{\tau_E}{\tau_Q} < \frac{G_{00}R_E + 1}{G_{11}R_pN - 1}\ . \quad (141)$$

To be more specific in calculations, the partial derivatives of the current components and some of their interrelationships are required. From Eq.(129) we get directly

$$G_{11} \equiv \frac{\partial I_{c1}}{\partial V_{b1}} = \alpha_f \frac{I_{ES} e^{V_{b0}/V_t}}{V_t} \; 2 \; \frac{d\hat{I}_1(x)}{dx} \; , \qquad G_{10} \equiv \frac{\partial I_{c1}}{\partial V_{b0}} = \alpha_f \frac{I_{ES} e^{V_{b0}/V_t}}{V_t} \; 2 \; \hat{I}_1(x) \; ,$$

$$G_{01} \equiv \frac{\partial I_{e0}}{\partial V_{b1}} = \frac{I_{ES} e^{V_{b0}/V_t}}{V_t} \; \frac{d\hat{I}_0(x)}{dx} \; , \qquad G_{00} \equiv \frac{\partial I_{e0}}{\partial V_{b0}} = \frac{I_{ES} e^{V_{b0}/V_t}}{V_t} \; \hat{I}_0(x) \; . \tag{142}$$

Comparisons between Eq.(142) and Eq.(5-95) show, that the effective fundamental frequency transconductance in oscillations is related to G_{10} through,

$$G_m = \frac{\alpha_f \, I_{ES} \, e^{V_{b0}/V_t}}{V_t} \; \frac{2 \, \hat{I}_1(x)}{x} = \frac{G_{10}}{x} \; , \qquad x = \frac{V_{b1}}{V_t} \; , \tag{143}$$

Therefore, fulfillment of Barkhausen´s condition links derivatives and circuit components by

$$G_m \, R_p \, N = 1 \quad \Rightarrow \quad G_{10} = \frac{x}{N R_p} \; . \tag{144}$$

Using the modified Bessel function identities, [9] 9.6.27,

$$\frac{d\hat{I}_1(x)}{x} = \hat{I}_0(x) - \frac{1}{x} \hat{I}_1(x) \, , \qquad \frac{d\hat{I}_0(x)}{dx} = \hat{I}_1(x) \, . \tag{145}$$

the complete set of partial derivatives is expressed

$$G_{11} = \alpha_f G_{ls} 2 \left(\hat{I}_0(x) - \frac{\hat{I}_1(x)}{x} \right) = 2 \, G_{00} - \alpha_f \frac{G_{10}}{x} \, , \qquad G_{10} = \alpha_f G_{ls} 2 \, \hat{I}_1(x) \, ,$$

$$G_{01} = G_{ls} \hat{I}_1(x) = \frac{G_{10}}{2 \, \alpha_f} \; , \qquad G_{00} = G_{ls} \hat{I}_0(x) \, , \tag{146}$$

$$\textit{where} \qquad G_{ls} \equiv I_{ES} \frac{e^{V_{b0}/V_t}}{V_t} \; .$$

Finally, the determinant of large signal transconductances becomes

$$\Delta \, G = G_{11} G_{00} - G_{10} G_{01} = \alpha_f 2 \, G_{ls}^2 \left(\hat{I}_0^{\,2}(x) - \hat{I}_1^{\,2}(x) - \frac{\hat{I}_0(x) \, \hat{I}_1(x)}{x} \right) , \tag{147}$$

This quantity is positive for all positive arguments x.

Positiveness of the determinant ΔG implies that the time constant condition in Eq.(141) always will be met choosing K_τ=1 if the inequality in Eq.(138) applies. Then the underlying requirement from Eq.(140) reads

$$\tau_Q \left[\; 1 + G_{00} R_E + 1 - G_{11} R_p N \; \right] \; > \; \tau_Q \left(\; 1 + \Delta G \, R_E R_p N \; \right) \; > \; 0 \quad ok! \tag{148}$$

Thus, setting the two time constants equal to each other gives a stable amplitude if the amplifier is self-limiting so all polynomials coefficients in the denominator from Eq.(135) are positive.

To gain more insight on circuit parameters, it is necessary to make the simplifying assumption, that the amplifier is driven strongly in class C. The larger argument x, the smaller relative difference between the modified Bessel functions, and we may estimate

$$\underline{large \;\; x}: \qquad G_{11} \approx G_{10} \approx 2\, G_{01} \approx 2\, G_{00} \approx \frac{x}{N R_p} \, . \tag{149}$$

One consequence of these assumptions is, that the determinant in of the derivatives looses significance, so the denominator coefficient of Eq.(135) are approximated,

$$A = \tau_Q^2 K_\tau \, , \qquad B = \tau_q \left[\; 1 + x \, \frac{R_E}{2 N R_p} - K_\tau \, (1 - x) \; \right] , \qquad C = 1 - x + x \, \frac{R_e}{2 N R_p} \, . \tag{150}$$

In the simplified version, the stability limit corresponding to Eq.(141) becomes

$$B > 0 \qquad \Rightarrow \qquad K_\tau = \frac{\tau_E}{\tau_Q} < \frac{x \, R_E / 2 N R_p + 1}{x - 1} \underset{large \, x}{\approx} \frac{R_e}{2 N R_p} \, . \tag{151}$$

Substituting for the time constants from Eqs.(130),(131) sets directly a bound on the decouplig capacitor C_E in terms of the tuning capacitor C

$$K_\tau = \frac{C_E R_E}{2 C R_p} < \frac{R_E}{2 N R_p} \qquad \Rightarrow \qquad C_E < \frac{C}{N} \, , \tag{152}$$

so to keep the oscillator free of squegging, the decoupling capacitor must be carefully selected and not just chosen from an "infinitely large" way of thinking.

Example VI-A-1 (amplitude stability)

By this example we shall employ the self-limiting class-C amplifier design from Example 5-3-1 in a 10 MHz prototype oscillator. Formerly the collector bias current was supplied separately by a RF-choke, L_{chk}, but the tuning inductor may be used for that purpose as well, as it is done by the circuit in Fig.46. Summarizing previous results, the amplifier has

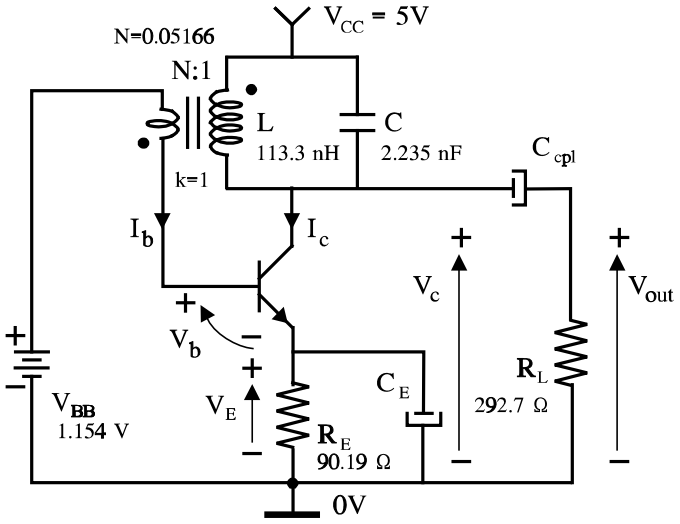

Fig.46 10 MHz prototype oscillator based on the class-C amplifier from Example 5-3-1. Output waveforms were shown in Fig.9 for two settings of C_E.

initial DC emitter current, transconductance, and voltage gain

$$\underline{x = 0:}$$

$$I_{e0} = I_{e00} = 5.043\,[mA]\ , \qquad g_m = \frac{\alpha_f I_{e00}}{V_t} = \frac{0.9836 \cdot 5.043 \cdot 10^{-3}}{0.025} = 0.1984\,[S] \tag{153}$$

$$A_{v0} = \left.\frac{V_L}{V_{b1}}\right|_{V_{v1} \ll V_r} = g_m R_p = .1984 \cdot 292.7 = 58.07\ .$$

With maximum input signal, V_{b1}=125 mV_{rms}, a gain reduction by a factor of three was required and the DC current, the transconductance, and the voltage gain change to

$$\underline{x = x_{max} = 7.071:}$$

$$I_{e0} = 6.416\,[mA]\ , \qquad G_m = \frac{g_m}{3} = \ = 0.06613\,[S], \qquad A_V = \frac{A_{V0}}{3} = 19.36\ . \tag{154}$$

To build an oscillator around this amplifier we must select the winding ratio of the feedback transformer so that Barkhausen's criterion is met. It gives

$$N = \frac{1}{G_m R_p} = \frac{1}{19.36} = 0.05166\ . \tag{155}$$

Using the results from Eqs.(5-95) and (5-100), the partial derivatives for the transistor current components evaluate to

$$G_{ls} = I_{ES} \frac{e^{V_{b0}/V_t}}{V_t} = 3.7 \cdot 10^{-15}\ \frac{e^{0.5747/0.025}}{0.025} = 1.425 \cdot 10^{-3} \tag{156}$$

$$
\begin{aligned}
G_{00} &= G_{ls}\hat{I}_0(x) = 1.425\cdot 10^{-3}\cdot 180.1 = 0.2566\ , \\
G_{10} &= \alpha_f G_{ls} 2\,\hat{I}_1(x) = .9836\cdot 1.424\cdot 10^{-3}\cdot 2\cdot 166.8 = 0.4676\ , \\
G_{01} &= \frac{G_{10}}{2\,\alpha_f} = \frac{0.4676}{0.9836\cdot 2} = 0.2377\ , \\
G_{11} &= 2\,G_{00} - \frac{\alpha_f G_{10}}{x} = 2\cdot 0.2566 - \frac{0.9836\cdot 0.4676}{7.071} = 0.4387\ .
\end{aligned}
\tag{157}
$$

Now the stability criterion from Eq.(141) gives an upper bound for stable time-constant ratios,

$$
K_{\tau,\max} = \frac{G_{00}R_E + 1}{G_{11}R_p N - 1} = \frac{0.2566\cdot 90.18 + 1}{0.4387\cdot 292.7\cdot 0.05167 - 1} = \frac{24.14}{5.635} = 4.286. \tag{158}
$$

This limit can be verified by simulations on both the amplitude control block-scheme in Fig.42 or by complete circuit simulations based on the diagram in Fig.46. Examples of the latter type were shown previously in Fig.9, where the lower, unstable case were a little above the limit, K_τ=4.5, in order to clearly demonstrate stationary oscillations. Deviating more severely from the stability limit gives unstable output waveshapes that in the audio frequency range sounds like the frogs squegging from which this type of instability was named. Fig.47 shows an example where K_τ=10.

The time constants τ_Q was calculated in Example 5-3-1, and the maximum limit becomes

$$
C_E\Big|_{stab.limit} = K_{\tau,max}\,\frac{\tau_Q}{R_E} = 4.286\cdot\frac{1.308\cdot 10^{-6}}{90.19} = 62.16[nF]\ . \tag{159}
$$

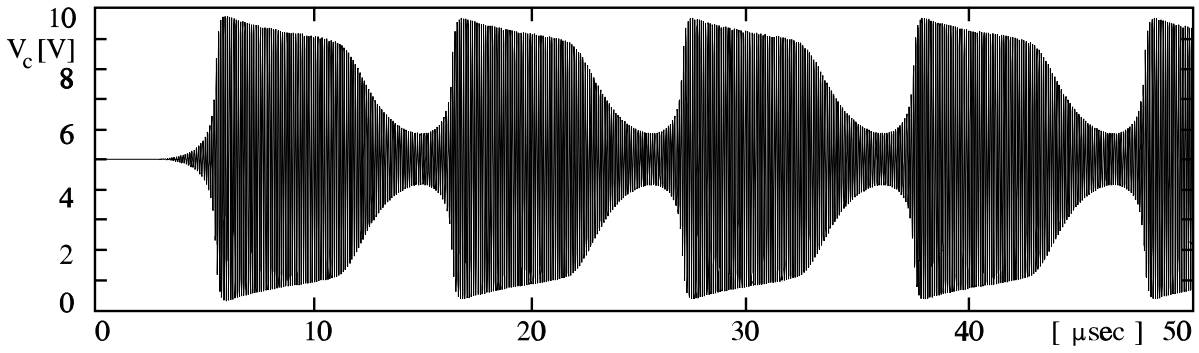

Fig.47 Oscillator output for K_τ=10 showing the characteristic 'squegging' waveform that has named this type of instability.

This result should be compared to the maximum value from the simplified analysis,

$$C_E\Big|_{stab.limit} = \frac{C}{N} = \frac{2.235}{0.05166} = 43.26[nF] \ . \tag{160}$$

As seen, we are on the safe side, but it is remarkable, that this simple solution to a complicated problem works. Going behind the result, it is observed that the correctly evaluated derivatives in Eq.(156) are in reasonable agreement with the simplifying assumptions from Eq.(150).

Example VI-A-1 end

Example VI-A-2 (amplitude stability with current bias)

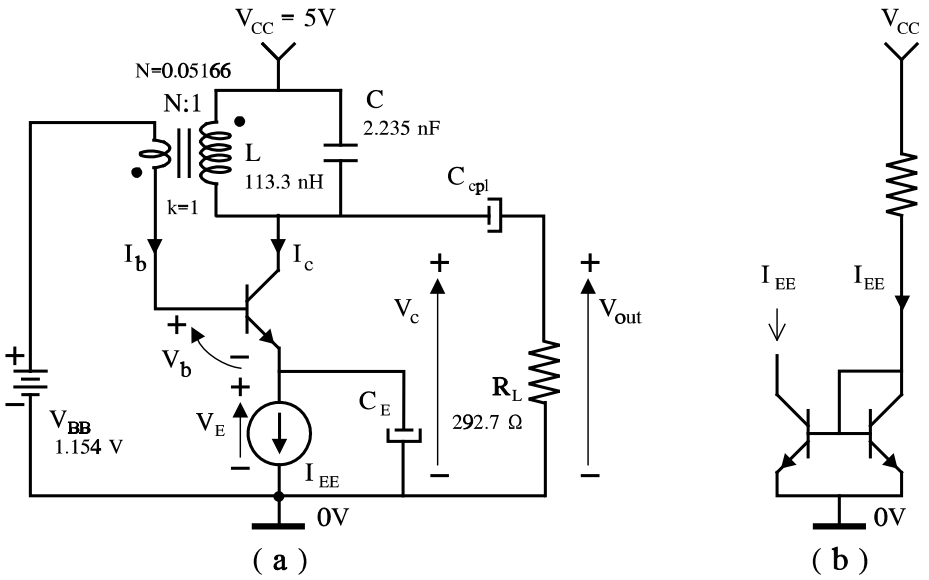

Fig.48 Simple feedback oscillator with current bias in common emitter configuration (a). Current biasing is often established by a current mirror (b).

Current biasing is an ideal way to get the self-limiting amplification, which is necessary for stabilizing the oscillator amplitude. The basic amplifier properties was discussed earlier in section 5-3, and Fig.48 shows its inclusion in the transformer feed-back oscillator that was discussed in the previous example. The large signal control of amplitude is now governed by the describing function block diagram in Fig.49, and its linearized counterpart is given by Fig.50. Compared to the similar schemes in the resistor biased case, Fig.42 and Fig.43, we get the linearized current biased scheme below as the limit of R_E approaching infinity in Fig.43.

Since the amplitude stability analysis formerly was based on the linearization, stability criteria for the present current biased oscillator are obtained from the resistor biased criteria as the limit case of R_E going to infinity. To do this, it is convenient to introduce a new time constant τ_{EE}. Instead of τ_E from Eq.(131) we use

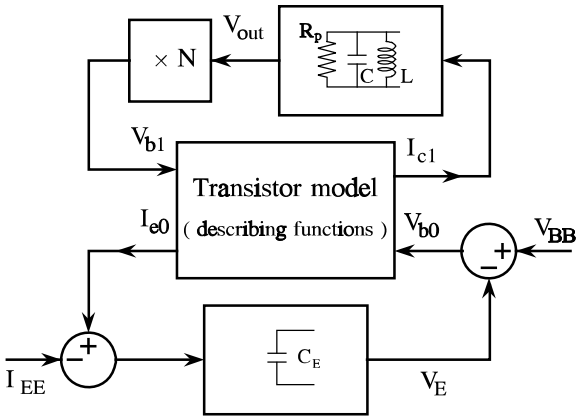

Fig.49 Block-diagram representation of oscillator amplitude control in a current biased oscillator like Fig.48.

$$\tau_{EE} \equiv C_E / G_{00} \ , \tag{161}$$

This time constant may be related to the current bias, since by Eqs.(5-99) and (142) we have

$$G_{00} = I_{EE} / V_t \ . \tag{162}$$

In the limit of $R_E \to \infty$, Eq.(135) reduces to

$$\begin{aligned} G_{\Delta 11}(s)\Big|_{R_E \to \infty} &= G_{11} \, \frac{c + bs + as^2}{C + Bs + As^2} \\ &= \frac{G_{11}\left(1 + s\left[\tau_{EE} + \tau_Q \right] + s^2 \tau_{EE} \tau_Q \right)}{1 - \Delta G \, R_p N / G_{00} + s\left[\tau_Q + \tau_E \left(1 - G_{11} R_p N \right) \right] + s^2 \tau_E \tau_Q} \ . \end{aligned} \tag{163}$$

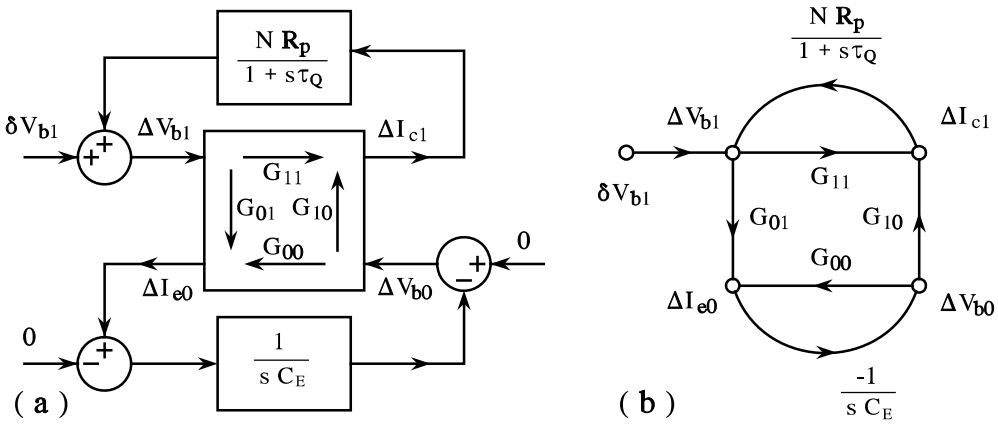

Fig.50 Linearization of the block-scheme from Fig.49 and the corresponding signal flow-graph.

To ensure stability, the B coefficient in the denominator must still be positive, and now the criterion reads

$$\underline{\textit{Amplitude Stability}\ (R_E \to \infty):} \qquad K_\tau \equiv \frac{\tau_{EE}}{\tau_Q} < \frac{1}{R_p N G_{11} - 1} \tag{164}$$

Under large drive conditions, where the approximations in Eq.(149) apply, we get the same upper bound on the decoupling capacitor C_E as we had before in Eq.(152), i.e.

$$C_E < \frac{\tau_Q G_{00}}{G_{11} R_p N - 1} \underset{large\ x}{\approx} \frac{C}{N} . \tag{165}$$

To demonstrate the usefulness of the criteria for current bias we consider the oscillator circuit in Fig.48. It is organized to resemble the resistor biased oscillator from Example VI-1-1 as close as possible, i.e. the normalized drive level x_{max} is maintained and the current bias I_{EE} is set equal to the former DC current from Eq.(154). Under such conditions the large signal transconductance G_m remains unchanged and Barkhausen's condition is fulfilled to provide the same output voltage that we had before with unchanged load R_p and winding ration N. Thereby, the stability bound becomes

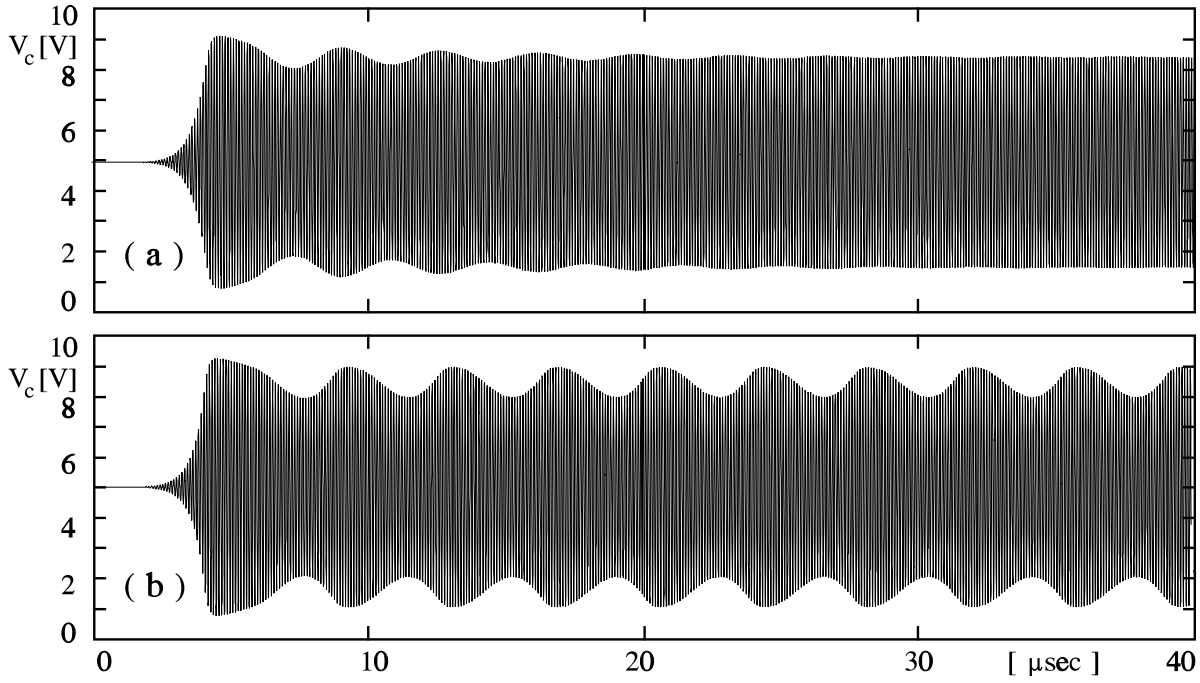

Fig.51 Outputs from the oscillator circuit in Fig.48. The upper and lower curves are at the stable and unstable side of the stability criterion with K_τ=0.1675 and 0.1875 respectively.

$$\frac{\tau_{EE}}{\tau_Q} < K_{\tau,max} = \frac{1}{R_p N G_{11} - 1} = \frac{1}{292.7 \cdot 0.05166 \cdot 0.4387 - 1} = 0.1775 \quad \Rightarrow \tag{166}$$

$$C_E < K_{\tau,max}\ \tau_Q\ G_{00} = 0.1775 \cdot 1.308 \cdot 10^{-6} \cdot 0.2566 = 59.57\,[nF]\ .$$

The two simulations below demonstrates the sharpness of the criterion by showing how the oscillations build up with K_τ = .1675 and .1875 respectively. In the first case the amplitude eventually stabilizes while in the second, spurious oscillations are sustained.

Example VI-A-2 end

Problems

P.VI-1

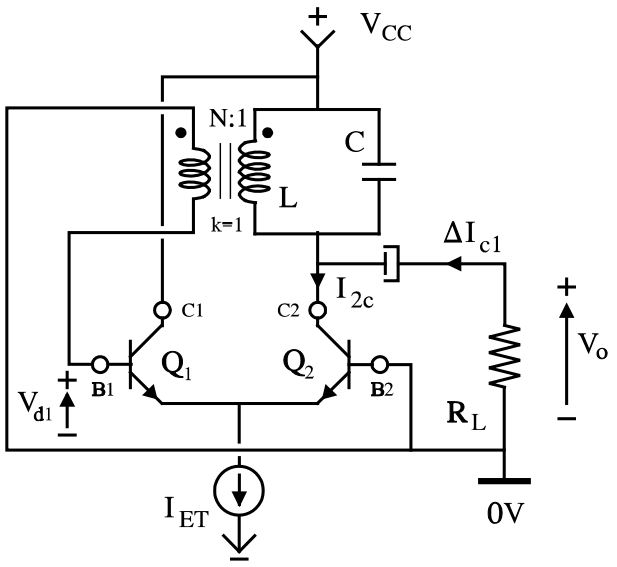

Fig.52

The oscillator in Fig.52 should be designed for maximum output at 2MHz without transistor saturation, i.e. keeping $V_{ce}\geq 0$. The supply voltage is V_{CC}=6V, the load resistor is R_L=800Ω. The inductance at the primary side of the transformer is L=2.5μH and a Q-factor of Q_L=50. The amplifier should be designed to show a gain reduction of 1:2.5 when oscillations build-up from initial small-signal to the required amplitude. Assume that transistor β_f is so high that the transistor input impedance may be ignored and that the base emitter voltage is 0.6V.

- Calculate the bias current I_{ET} and the small-signal gain g_{md}.
- Find the transformation ratio N and capacitor C.
- Estimate the total harmonic distortion of the output voltage.

P.VI-2

Fig.53 shows a Colpitts oscillator circuit with a bipolar transistor. At the oscillating frequency, the transistor base and the collector supply are AC-grounded through the decoupling capacitors C_{cp1} and C_{cp2}. C_{cp3} is a coupling capacitor and resistors R_{b1}, R_{b2}, and R_E are bias resistors. Inductor L_{rcf} is a bias choke that may be considered infinitely large in design. The tuning components are C_A, C_B, and L_C. They are all assumed lossless.

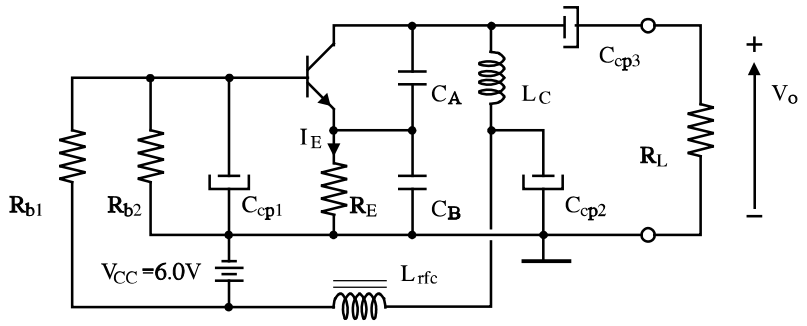

Fig.53 Colpitts Oscillator Circuit

The circuit should be designed to meet the following requirements,

- frequency, f_0 = 20 MHz,
- output voltage V_o = 1.5 V_{rms} in R_L= 200Ω,
- loaded Q-factor, Q_l > 25,
- gain reduction at nominal output, G_m:g_m ~ 1:3.5

It is supposed that the transistor requires V_{ce} > $V_{ce,min}$=0.5V to prevent saturation effects, that it has a forward current gain β_f = 80, and that its base-emitter voltage in small-signal operation is 0.80V.

Calculate all component values of the circuit in Fig.53. Assume in the initial steps of the design that the transistor is current biased and find the bias current I_E. Afterwards, R_E should be chosen as high as possible to approximate the current bias conditions.

P.VI-3

Consider a crystal operated in series resonance with resonance frequency f_0. Show that the frequency where the impedance becomes real differs from f_0 by

$$\Delta f = \frac{f_0}{2Q}\frac{C_0}{C_1 Q} = \frac{f_0}{2Q}\frac{1}{M}, \qquad (167)$$

if the electrode capacitance C_0 is accounted for in details. Explain why the frequency difference is insignificant.

P.VI-4

Fig.54 shows a Pierce crystal oscillator. It is supposed that the crystal is the 10 MHz crystal from Eq.(111) with a series capacitance of C_{ser}=22 pF. The crystal and the series capacitor replaces the inductance L_C in the oscillator design from Example VI-2-2 on page 29. All other components are kept unchanged.

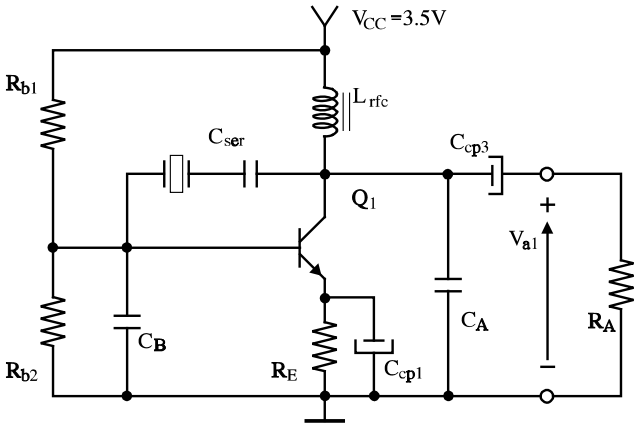

Fig.54

Calculate the output voltage, the oscillator frequency, and the loaded Q-factor of the oscillator in Fig.54.

P.VI-5

Fig.55 shows a Pierce crystal oscillator. It is supposed that the crystal is the 10 MHz crystal from Eq.(111) used in series, impedance inverting mode like Fig.40(b) with inductance L_C. The rest of the circuit is the oscillator design from Example VI-2-2 on page 29, and all components values are kept unchanged from the example.

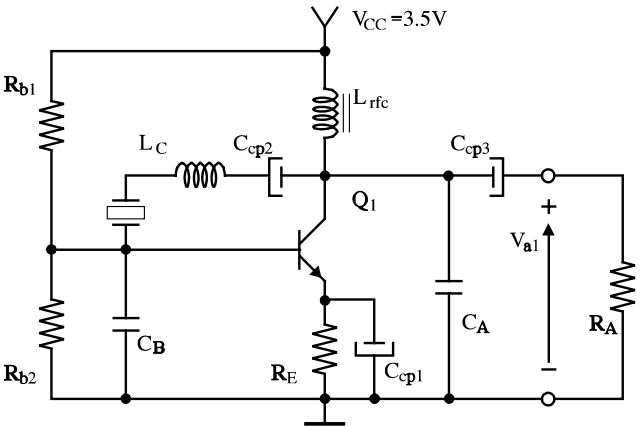

Fig.55

Calculate the output voltage, the oscillator frequency, and the loaded Q-factor of the oscillator in Fig.55.

References and Further Reading

[1] N.M.Nguyen, R.G.Meyer,"Start-up and Frequency Stability in High-Frequency Oscillators", IEEE Journ.Solid-State Circuits, Vol.SC-27, pp.810-820, May 1992. Included in [2].

[2] B.Razavi,ed., Monolitic Phase-Locked Loops and Clock Recovery Circuits, Theory and Design, IEEE Press 1996, Selection of 65 papers including approximately 10 on oscillator design and properties.

[3] R.S.Elliott, An Introduction to Guided Waves and Microwave Circuits, Prentice-Hall 1993.

[4] G.Gonzalez, "Microwave Transistor Amplifiers" 2nd ed. Prentice-Hall 1997.

[5] D.B.Leeson, "A simple Model of Feedback Oscillator Noise Spectrum", Proc.IEEE, Vol.54,Feb.1966,pp.329-333. Included in [2].

[6] E.Hafner, "The Effect of Noise in Oscillators", Proc.IEEE, vol.54, pp.179-198, Feb.1966. Included in [2].

[7] A.van der Ziel, Noise in Solid State Devices and Circuits, Wiley 1986.

[8] M.E.Frerking, Crystal Oscillator Design and Temperature Compensation, Van-Nostrand 1978.

[9] M.Abromowitz,I.A.Stegun, Handbook of Mathematical Functions, Dover,NY, 1965

Index